Quaternary Science Reviews 252 (2021) 106739

Contents lists available at ScienceDirect

Quaternary Science Reviews

journal homepage: www.elsevier.com/locate/quascirev

Holocene regional population dynamics and climatic trends in the Near East: A first comparison using archaeo-demographic proxies

Alessio Palmisano [a, b, *], Dan Lawrence [b], Michelle W. de Gruchy [b], Andrew Bevan [c], Stephen Shennan [c]

[a] Department of Ancient History, Ludwig Maximilian University of Munich, Geschwister-Scholl-Platz 1, Munich, 80539, Germany
[b] Department of Archaeology, Durham University, South Road, Durham, DH1 3LE, United Kingdom
[c] Institute of Archaeology, University College London, 31-34 Gordon Square, London, WC1H 0PY, United Kingdom

ARTICLE INFO

Article history:
Received 22 May 2020
Received in revised form
18 October 2020
Accepted 24 November 2020
Available online 19 December 2020

Keywords:
Climate dynamics
Paleodemography
Holocene
Middle East
Speleothems
Radiocarbon summed probability distribution
Archaeological survey

ABSTRACT

This paper illustrates long-term trends in human population and climate from the Late Pleistocene to the Late Holocene (14,000–2500 cal. yr. BP) in order to assess to what degree climate change impacted human societies in the Near East. It draws on a large corpus of archaeo-demographic data, including anthropogenic radiocarbon dates (n = 10,653) and archaeological site survey (n = 22,533), and 16 hydro-climatic records from cave speleothems and lake sediments. Where possible, inferred population dynamics and climatic trends have been made spatially congruent, and their relationships have been statistically tested. Demographic proxies and palaeoclimatic records have been compared for the greater Near East as a whole and for seven major geo-cultural regions (Anatolia, Arabia, Cyprus, Iran, Levant, Mesopotamia, and South Caucasus). This approach allows us to identify regionalised patterns in population and climate trends. The results suggest a clear relationship between population and climate in the Late Pleistocene and Early Holocene (14,000–8326 cal. yr. BP) with population increasing in concomitance with wetter climatic conditions. During the Middle Holocene (8326-4200 cal. yr. BP) there is an increased regionalisation of demographic patterns, followed by marked interregional contrasts in the Late Holocene (4200-2500 cal. yr. BP). We identify a decoupling of demographic and climatic trends from the Middle Holocene onwards, and relate this to the existence of more complex societies. These were less vulnerable to gradual climatic shifts due to their logistical infrastructure, social organisation and technological capacity. We also assess the impact of five Rapid Climate Changes (RCC) which occurred during the study period on population levels. Although all five RCC (the so-called 10.2 k, 9.2 k, 8.2 k, 4.2 k, and 3.2 k cal. yr. BP events) are visible to some degree in our palaeoclimatic and demographic proxies, there are marked regional variations in magnitude and duration.

1. Introduction

Population growth occupies a central role in public debate due to its implications for subsistence strategies, environmental change, and migration, and its relationship with exogenous factors such as climate variations. In the archaeological and anthropological debate, population has been identified as a driver for cultural change (Naroll, 1956; Carneiro, 1962) and an explanation for variation in subsistence strategies (Boserup, 1965; Binford 1968; Shennan 2000; Peregrine 2004), social complexity (Johnson and Earle 2000; Feinman 2011), socioeconomic outputs (Bettencourt et al., 2007; Ortman et al., 2014; Altaweel and Palmisano 2019; Smith 2019) and intra-group conflicts (Goldstone 1993; Kohler et al., 2009; Turchin and Nefedov 2009). More recently, interest in human-environment interactions has prompted an increasing number of studies investigating the impact of human population on landscape, including to what degree population fluctuations were affected by climatic shifts (Langgut et al., 2016; Lawrence et al., 2016; Kaniewski and Van Campo 2017; Bevan et al., 2019; Roberts et al., 2019; Stephens et al., 2019). Building past human population models over the longue durée (and assessment of the causes of

* Corresponding author. Department of Archaeology, Durham University, South Road, Durham, DH1 3LE, United Kingdom.
E-mail addresses: alessio.palmisano@lrz.uni-muenchen.de, a.palmisano82@hotmail.com (A. Palmisano), dan.lawrence@durham.ac.uk (D. Lawrence), michelle.de-gruchy@durham.ac.uk (M.W. de Gruchy), a.bevan@ucl.ac.uk (A. Bevan), s.shennan@ucl.ac.uk (S. Shennan).

https://doi.org/10.1016/j.quascirev.2020.106739

fluctuations) is critical for our understanding of cultural and environmental changes at a range of scales.

In this context, the Near East represents an excellent laboratory in which to investigate long-term relationships between demographic and climatic trends. This area is a mosaic of different cultural and environmental landscapes, which each experienced linked but different socio-ecological trajectories (Wilkinson 2003; Rosen 2007; Ur 2009, 2015; Roberts et al., 2011; Wilkinson et al., 2014; Izdbeski et al., 2016; Lawrence et al., 2017; Jones et al., 2019; Palmisano et al., 2019; Woodbridge et al., 2019). It also endured pronounced regional dry/wet episodes during the Late Pleistocene and Holocene which would have impacted on human behaviour (Burstyn et al., 2019; Jones et al., 2019).

The rise and fall of population and the emergence or collapse of complex societies has been attributed to shifts in climatic regimes. For example, the Younger Dryas stadial (~12,700–11,700 cal. yr. BP), a period of increased aridity and cooling, has been interpreted as a cause for a reduction in site occupation intensity (Belfer-Cohen and Bar-Yosef 2000; Guerrero et al., 2008; Goring-Morris and Belfer-Cohen 2010) and as a driver towards more productive techniques in plant cultivation as a response to declining natural sources (Cappers et al., 2002). A recent study by Roberts et al. (2018) showed that neolithisation and population increase occurred in the Fertile Crescent earlier than in the Anatolian plateau, and argued that this delay was caused by more favourable climatic conditions in the former area during the climatic deterioration of the Younger Dryas stadial (~12,700–11,700 cal. yr. BP). The uneven impact of these climatic shifts across the whole Near East could explain local cultural variations manifesting at different speeds and magnitudes. Some trends are also visible at pan-regional scales. For example, studies focused on Anatolia, Northern Mesopotamia and the Southern Levant have all suggested that from 4000/3500 cal. yr. BP onwards demographic trends become decoupled from those of climate, perhaps due to the technological advancement, organisational capacity and logistical infrastructure of more complex societies which makes populations more resilient to drought and food stress (Rosen 2007; Lawrence et al., 2016; Roberts et al., 2019). Alongside these longer-term trajectories, the Near East experienced several major rapid climate changes during the Holocene (RCC, the so-called 10.2 k, 9.2 k, 8.2 k, 4.2 k, and 3.2 k cal. yr. BP events). These are also considered to have affected demographic trends and triggered social responses, although there is much debate on the degree and nature of these. The 10.2 k cal. yr. BP event could be a factor in a cultural break visible across the Northern Levant and Upper Mesopotamia (Borrell et al., 2015). A consensus is beginning to emerge around the 9.2 k and 8.2 k cal. yr. BP events suggesting that they had a more limited impact on Near Eastern communities (Flohr et al., 2016; Allcock 2017), but the 4.2 k. cal. yr. BP event has prompted an animated debate, with some scholars arguing it was responsible for massive population decline and societal collapse (Weiss et al. 1993, 2017; Kaniewski et al., 2018) and other preferring more nuanced views (Wilkinson 1997, 2007; Roberts et al., 2011; Greenberg 2017; Cookson et al., 2019). There is a broader agreement on the role of the 3.2 k cal. yr. BP event as a major driver of political and social collapse (Langgut et al., 2013; Cline, 2015; Izdebski et al., 2016; Kaniewski et al. 2015, 2019).

In this paper, we draw upon a large corpus of archaeological data (in the form of settlements from archaeological surveys and radiocarbon dates) and palaeoclimatic records across the whole Near East in order to provide the first systematic empirical analysis on a pan-continental scale in the very long run. Our assumption is that, all other factors remaining constant, increased aridity will negatively affect soil moisture, and therefore vegetation, food production and human population. However, this relationship is not straightforward, and is mitigated by human responses to change, including social and technological adaptation and population movement. The goal of the paper is to examine to what degree climate and population trends correlate with one another. In order to do this we compare trends visible in the summed probability distributions (SPD) of calibrated radiocarbon dates with several palaeoclimatic records. We also test the robustness of the SPD generated trends by comparing them with more traditional archaeological proxies for population (raw site count and estimated settled area) in three sub-regions. With some exceptions, studies concerning population patterns in the Near East have tended to focus on relatively small areas and short time periods. Here we include the entirety of the greater Near East in the radiocarbon dataset, from the Arabian Peninsula to the South Caucasus, including Anatolia, the Levant, Mesopotamia and Iran. Chronologically we range from the Late Pleistocene to the Late Holocene (ca. 14,000–2500 cal. yr. BP). The three sub-regions used for comparison are determined by the availability of collated high-quality archaeological survey data. They include South-central Anatolia, Upper Mesopotamia and the Southern Levant. The fluctuations in demographic and climatic variables are quantitatively assessed to examine the correlation between the different demographic proxies, the correlations between climate change and population dynamics through time, and the impact of RCC events.

2. Geographical setting and materials

2.1. The study area

The Near East is a large area with a diversity of landscapes and climate regimes, including fertile drylands, alluvial plains, coastlands, high mountain chains and extensive deserts. Most of the area experiences warmer summers and colder winters, with rainfall occurring in the winter. Extremely dry conditions prevail in the southern part of the region, the Arabian Peninsula, which is mostly arid except in the highlands of Yemen and Oman where precipitation is increased by the Indian Monsoonal system (Enzel et al., 2015; Jones et al., 2019). The coasts of the Mediterranean and Black Seas, the Levant and Anatolia enjoy relatively abundant rainfall and rich agricultural lands (Fisher 2013). Across the entire region there are a series of marked average annual rainfall gradients, with values exceeding 2000 mm in the Caucasus and Zagros Mountains but less than 100 mm in the Arabian Peninsula and Southern Negev (Hemming et al., 2010; Lelieveld et al., 2012).

In order to deal with this variation, we have subdivided the Near East into seven major geo-cultural regions (Anatolia, Arabia, Cyprus, Iran, Levant, Mesopotamia, and South Caucasus; see Fig. 1). The regional classification is still very broad, and each area encompasses a range of landscapes. In delineating our study areas, we have attempted to balance regional scale and relative geographical and cultural homogeneity, with sufficient data coverage for archaeo-demographic proxies, particularly radiocarbon dates, to be effective. The geographical extent of our regions, from the Eastern Mediterranean to the Indus valley and from the Black Sea to the Arabian Sea, allows us to compare regionalised patterns of population and climate. While we have attempted to guarantee spatial and temporal congruence between the demographic and climatic records, this has not always been possible due to the distribution of paleoclimate records and archaeological data. Several of our climate records do not cover the entire chronological scope from the Late Pleistocene to the Late Holocene (14,000–2500 cal. yr. BP), but given the paucity of resources in the region we have included all those currently available in a quantified form. In this study, we refer to the triplex subdivision of the Holocene established by the International Commission on Stratigraphy (Walker et al., 2018): Early Holocene/Greenlandian (11,700–8326 cal. yr. Bp), Middle

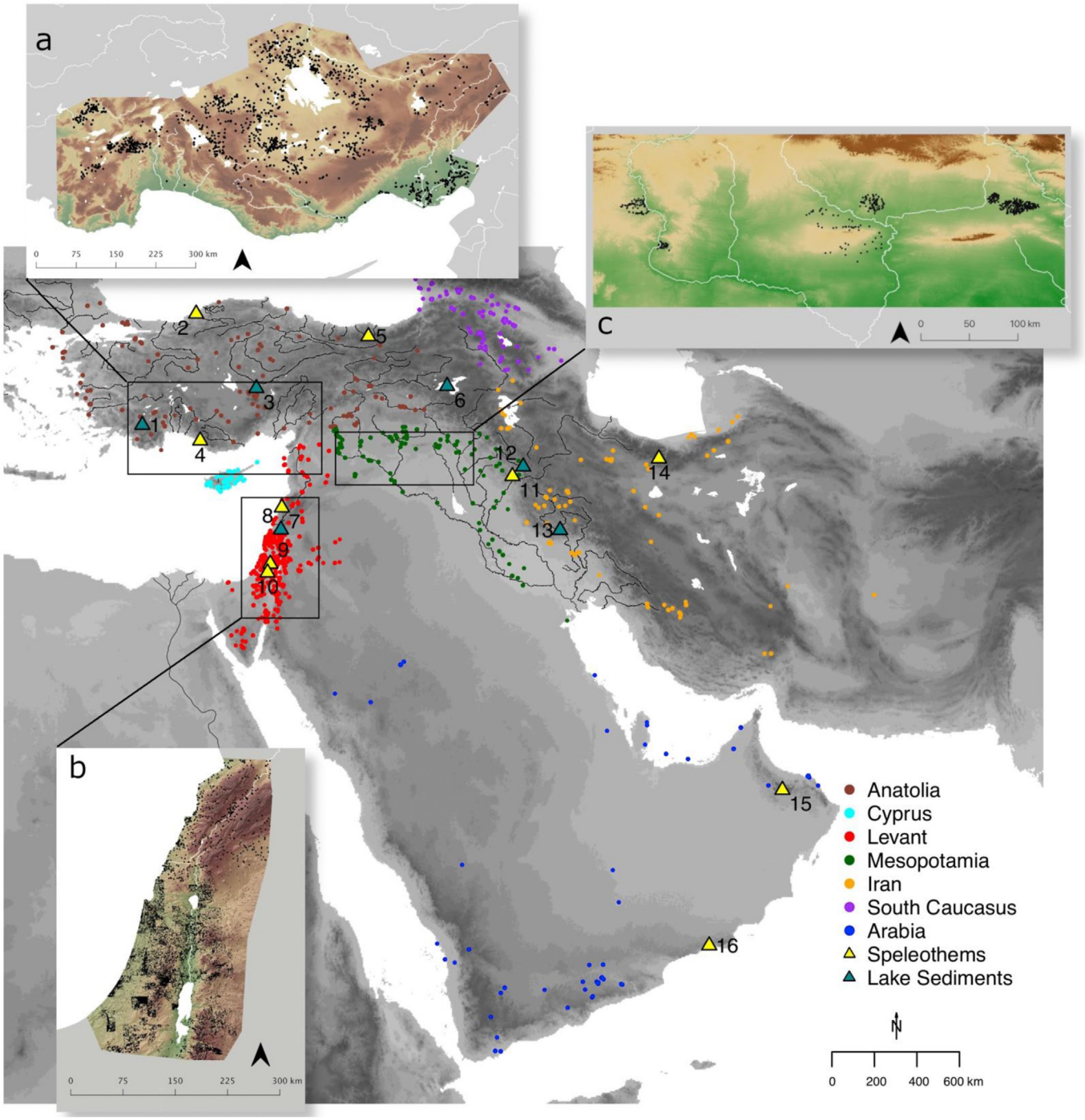

Fig. 1. Study area and spatial distribution of radiocarbon dates. Settlements data from a) South-central Anatolia, b) southern Levant, and c) Upper Mesopotamia.

Holocene/Northgrippan (8326–4200 cal. yr. BP, and Late Holocene/Meghalayan (4200 cal. yr. BP – 1950 AD).

2.2. Archaeo-demographic proxies

Population estimates build on the assumption that the density of the archaeological evidence found in a given study area is proportional to population (see Drennan et al., 2015 for a useful overview). The most popular proxies for inferring long-term changes in human populations in the Near East have been raw counts of archaeological sites and sums of estimated settlement sizes. These are commonly derived from archaeological field investigation such as landscape survey or site mapping (e.g. Sanders 1965; Adams 1965, 1981; Wright and Johnson 1975; Gophna and Portugali 1988; Finkelstein and Gophna 1993; Wilkinson 1999; Casana 2009; Ur 2013; Lawrence et al., 2016, 2017). Over the past two decades, SPDs of archaeological radiocarbon dates have begun to be used to infer demographic trends in prehistory (see Rick 1987; Shennan and Edinborough 2007; Weninger et al., 2009; Shennan et al., 2013; Silva and Vander Linden, 2017; de Pablo et al., 2019). These approaches have had limited impact in the Near East, and where attempted have focused

on single regions or very specific time periods (cf. Borrell et al., 2015; Flohr et al., 2016; Palmisano et al., 2019; Woodbridge et al., 2019). Here we make use of a total of 10,653 radiocarbon dates from 993 sites collected from existing online digital archives (ArAGATS project: 2019; BANADORA: CDRC 2016; Borrell et al., 2015; CalPal: Weninger et al., 2018; CONTEXT: Böhner and Schyle 2006; EUROEVOL: Manning et al., 2016; Flohr et al., 2016; IRPA/KIK: Van Strydonck and De Roock 2011; ORAU , 2016; PPND: Benz 2014; RADON: Hinz et al., 2012; TAY project: 2019; 14SEA: Reingruber and Thissen 2017), and electronic and print publications. To our knowledge, this is the largest collation of published radiocarbon dates for the Near East. We have not been able to include unpublished dates or those published in non-digital grey literature. Wherever possible the radiocarbon dates were cross-checked against different sources and georeferenced consistently (see Fig. 1). All the radiocarbon dates come from archaeological contexts and most of them are taken from samples of bone, charcoal, and seeds (see Table 1). Radiocarbon dates with poorly understood marine reservoir offsets (all shells), a standard error greater than 300 years, or that do not have anthropogenic causes (e.g. radiocarbon samples collected from environmental cores) have been excluded and are not part of the above total. The total number of dates exceeds the minimum sample size of 200–500 required to produce reliable SPDs of calibrated radiocarbon dates within a time interval of 8–10,000 years (Michczyńska and Pazdur, 2004; Michczyńska et al., 2007; Williams, 2012, 580–581). As a consequence, our dataset can be considered to be sufficiently large to overcome many of the potential sampling biases that might affect the patterns. The SPDs of calibrated radiocarbon dates are effective until 3000/2500 cal. yr. BP because after that archaeologists rely more on short-lived pottery types for dating archaeological layers. This period is also affected by the Hallstatt radiocarbon calibration plateau (ca. 2750–2350 cal. yr. BP) which makes it difficult to obtain refined radiocarbon-based chronologies.

Both archaeological survey data (raw count, estimated settlement size) and radiocarbon dates are imperfect proxies and are subject to several issues that may affect the relationship between the archaeological data and past population levels. These include biases in research focus towards particular periods or regions, variations in the methods adopted and the intensity of the investigation, taphonomic loss and the visibility of diagnostic artefacts (Cherry 1983; Surovell et al., 2009; Contreras and Meadows 2014; Torfing 2015, 2016; Becerra-Valdivia et al., 2020). The generation of SPD datasets requires excavation and sampling for radiocarbon dating. In areas of the world such as the Near East where modern states do not routinely integrate archaeological work into their planning and construction industries, the majority of archaeological excavation is driven by academic research projects and their attendant interests. As a result, such areas may be more affected by the concentration of research on particular topics, such as the emergence of farming, which in turn emphasises particular periods, than areas with a long tradition of commercial archaeology. This is less of a problem for archaeological surveys, which generally attempt to capture all sites within a landscape regardless of period (unfortunately often with the exception of very recent occupation). Unlike survey, SPDs do not capture variables such as site size or type. Expansion in the size of sites can lead to a counter-intuitive state of affairs in which the number of sites reduces but the population likely increased. This occurred in Southern Mesopotamia during the period of initial urban emergence from 6000 cal. yr. BP (Adams 1981), and in some areas of Upper Mesopotamia during the Early Bronze Age (Lawrence and Wilkinson 2015). However, SPDs of calibrated radiocarbon dates generally provide a better chronological resolution than artefactual data because the latter rely on the identification of changes in lithic and ceramic assemblages to define chronological periods and these changes may occur relatively slowly. Archaeological surveys which rely on surface collection cannot include stratigraphic information or data on proportions of pottery types, resulting in further chronological imprecision.

Despite these issues, several studies have shown broad agreement in the demographic trends produced by the SPD of radiocarbon dates and other archaeological indices (e.g. raw site count, estimated settlement size) (Tallavaara et al., 2010; French 2015; French and Collins 2015; Demjan and Dreslerová 2016; Palmisano et al., 2017; Nielsen et al., 2019). The "Changing the Face of the Mediterranean" project, a Plymouth University-UCL collaboration, has confirmed that SPDs can be regarded as a robust proxy for modelling past human population in a region adjacent to our study area (see Bevan et al., 2019; Berger et al., 2019; Palmisano et al., 2019; Roberts et al., 2019; Stoddart et al., 2019; Weiberg et al., 2019). Here we assess the limitations of the different proxies through a cross-comparison between multiple archaeo-demographic proxies. Archaeological site derived proxies (site count, settlement size) are compared to the SPD of calibrated radiocarbon dates for three sub-regions, South-central Anatolia, the Southern Levant and Upper Mesopotamia, to develop a better understanding of long-term population dynamics (see Table 1). The sub-regions were chosen because they have sufficient high quality systematic archaeological survey data to assess general trends. A fourth sub-region which has a similar archaeological survey dataset in our study region is Southern Mesopotamia, but here the paucity of excavation since the early 1990s means the number of published radiocarbon dates falls below the threshold for robust analysis. The majority of the cited papers where analogous work has been undertaken focus on relatively homogenous fertile lowland environments, and our study regions are similar. This means they are a poor test of the validity of the SPD data for dissimilar environments such as desert Arabia or mountainous Eastern Anatolia and the Caucasus, which also had rather different settlement histories. Further work is needed to bring together archaeological settlement datasets in these regions of sufficient size and scale to compare to the SPD record. However, SPDs are beginning to be used in some of these regions (Petraglia et al., 2020), and in the absence of appropriate

Table 1
Summary of the archaeo-demographic proxies for each case study region. See Fig. 1 for the spatial extent of the three sub-regions South-central Anatolia (a), Southern Levant (b), and Upper Mesopotamia (c).

Region	^{14}C dates (n)	Site numbers	Site areas	Sub-regional division
Anatolia	2640	Only for a selected sub-region (1336)	Only for a selected sub-region	South-central Anatolia
South-Caucasus	665	No	No	NA
Cyprus	494	No	No	NA
Levant	3843	Only for a selected sub-region (20,688)	No	Southern Levant
Mesopotamia	1587	Only for a selected sub-region (509)	Only for a selected sub-region	Upper Mesopotamia
Iran	1019	No	No	NA
Arabia	405	No	No	NA

settlement datasets we would argue that they can act as an empirically derived heuristic device for examining the causal relationship between climate change and population. This is not to claim that SPDs of radiocarbon dates are a more appropriate proxy than archaeological survey data for population. We use them here due to their wider spatial and temporal availability, and chronological precision. Ideally we would use both archaeo-demographic proxies throughout the whole study area and for the entire study period, but settlement datasets at these scales are not yet available.

The archaeological settlement data for South-central Anatolia and Upper Mesopotamia were collected and harmonised from reports and gazetteers of archaeological surveys of varying intensity (see the Appendix B for references). Settlement data were recorded as geo-referenced points (unprojected WGS84) per standardised cultural periods, which have been defined in absolute calendric years to provide maximum comparative potential among archaeological sites. Here we include those places identified as habitation sites or possible habitations and have removed sites such as cemeteries or mines where no evidence of settlement was recovered. The archaeological survey data cover a period spanning from 10,000–2500 cal. yr. BP as, unlike the radiocarbon dates, there are insufficient data for the earlier periods. We recorded a total of 1336 sites and 3543 occupation phases for south-central Anatolia and 509 sites divided into 1772 site-phases for Upper Mesopotamia (Table 1 and Fig. 1: a, c; see the Appendix B for the full list of archaeological surveys). A total of 20,688 sites and 66,183 occupation phases were collected for the Levant and then standardised from two extant online databases: 1) The Digital Archaeological Atlas of the Holy Land (Savage and Levy 2014), and 2) The West Bank and East Jerusalem Archaeological Database (Greenberg and Keinan 2009). One major caveat in this latter dataset is that the estimated size of settlements for each cultural period was not consistently available, and therefore we have only used the raw site count as a proxy for the population.

2.3. Palaeoclimatic records

For simplicity, in the present study we have used a palaeoclimatic proxy reflecting past hydro-climatic patterns and omitted those proxies indicating variability in temperature or pollen-based climate reconstructions. We have only included datasets where full results have been published and raw data are available. The palaeoclimatic dataset includes 16 stable oxygen isotope ratios ($\delta^{18}O$) of speleothems and lake sediments collected from different regions (see Fig. 1 and Table 2) which provide relative precipitation levels. In the arid and semi-arid regions which make up most of the study area, we expect precipitation levels to correlate closely with vegetation and surface water availability (Jones et al., 2019). Although the spatial coverage of the available records is heterogeneous, with some areas such as Cyprus and the central part of the Fertile Crescent lacking natural palaeoclimatic archives, it is possible to identify regional climate variability across the whole Near East. A further issue to bear in mind is that most of our palaeoclimatic records (12 out of 16) are located at more than 650 m above sea level and reflect past climatic conditions in upland landscapes (see Table 2), while most of our archaeological data comes from lowland basins.

Stable oxygen isotopes from caves and lakes are used as hydrological indicators due to their rapid response to changes in water availability, and their fine-grained temporal resolution based on radiocarbon or uranium-series dating (Bar-Matthews et al., 2003; Fleitmann et al., 2007; Finné et al., 2017). The higher and lower values of stable oxygen isotopes indicate respectively drier and wetter conditions. However, the interpretation of $\delta^{18}O$ values is not always straightforward as they can be affected by several environmental factors (e.g. vegetation, recharge conditions, open water evaporation) occurring in the original context of a given record. In addition, some authors have recently suggested that the $\delta^{18}O$ of the speleothem calcite represents the precipitation amount of the winter season rather than average annual conditions (Wassenburg et al., 2016; Deininger et al., 2017; Bini et al., 2019), and there is no unifying explanation for values across the Mediterranean basin (Moreno et al., 2014). A recent study by Baker et al. (2019) has highlighted that those sites from regions (eg. Northern Europe, northern America) with an annual mean temperature less than 10 °C have an oxygen isotope composition strongly related to the isotopic composition of local rainfall. Instead, those regions, such as the Mediterranean basin and Near East, with an annual mean temperature between 10 and 16 °C, can be more susceptible to moisture balance change due to the evaporative fractionation of stored karst water and selective recharge. Conversely, the $\delta^{18}O$ values of lacustrine carbonate are believed to correlate with hydroclimate conditions during summer (Leng and Marshall 2004; Bini et al., 2019) although more complex explanations have been proposed (Zielhofer et al., 2019). These palaeoclimatic records can be sensitive to air mass trajectories and to shifts in evaporative concentration.

It is not the main goal of this paper to describe in detail the uncertainties of each climate record, and several recent reviews provide excellent syntheses of the available data (Roberts et al., 2008; Burstyn et al., 2019; Finné et al., 2019; Jones et al., 2019). We invite the reader to refer to these and the original publications for detailed descriptions of each record (see Table 2). All the palaeoclimatic records of this study were collected from existing online repositories and databases (NOAA; SISAL database: Atsawawaranunt et al., 2019). We selected those records which were freely accessible online, could provide reasonable spatial coverage and included multimillennial time duration across the Holocene. While some records have a fine and detailed chronology (for example, Jeita and Sofular caves) other ones have a mean sampling interval greater than 200 years (for example Jerusalem West cave and Lake Zeribar).

3. Methods

In this paper we draw on developed methods to infer past population dynamics from archaeological settlements data (Palmisano et al., 2017) and to test statistically the SPDs of calibrated radiocarbon dates (cf. Shennan et al., 2013; Timpson et al., 2014; Crema et al., 2016; Bevan et al., 2017). We provide here a general description of those methods, which are explained in detail in the original publications. All analyses and figures are reproducible thanks to the dissemination of the datasets and four scripts written in R statistical computing language (Appendix A).

3.1. Archaeology settlement data derived proxies

The archaeological settlement data (raw site count, aggregated estimated settlement size) have been binned into a series of 200-year time slices starting at 10,000 cal. yr. BP (period t_1: 10,000–9800 cal. yr. BP) and ending at 2600 cal. yr. BP (period t_{37}: 2800-2600 cal. yr. BP). Because the length of cultural periods varies according to the precision of the dating of archaeological artefacts (e.g. pottery), with the earlier periods often spanning hundreds of years, we applied aoristic analysis to deal with the temporal uncertainty of occupation periods and generated aoristic weights (for a more detailed explanation of the methodology see Crema et al., 2010, 1118–1121; Crema 2012, 446–448; Palmisano et al., 2017,

Table 2
List of palaeoclimate records.

Map no.	Site name	Archive	Proxy	Longitude	Latitude	Elevation (masl)	Chronological Coverage (cal. yr. BP)	Reference
1	Lake Gölhisar	lake sediments	$\delta^{18}O$	29.6	37.13	930	10,559-302	Eastwood et al., (2007); Roberts et al., (2008)
2	Sofular cave	speleothem	$\delta^{18}O$	31.93	41.42	700	50,275-present	Fleitmann et al., (2009); Shah et al., (2013)
3	Eski Acıgöl	lake sediments	$\delta^{18}O$	34.54	38.55	1270	20,381-1444	Roberts et al., (2001) and 2008
4	Dim cave	speleothem	$\delta^{18}O$	32.11	36.53	232	13,094-9738	Ünal-İmer et al., (2015); Atsawawaranunt et al., (2019)
5	Karaca cave	speleothem	$\delta^{18}O$	39.40	40.54	1536	77,300-5904	Rowe et al., (2012); Atsawawaranunt et al., (2019)
6	Lake Van	lake sediments	$\delta^{18}O$	42.81	38.63	1648	16,128-56	Wick et al., (2003); Roberts et al., (2008)
7	Jeita cave	speleothem	$\delta^{18}O$	35.65	33.95	100	20,367-372	Cheng et al. (2015)
8	Lake Hula	lake sediments	$\delta^{18}O$	35.6	33.10	60	15,105–205	Roberts et al. (2008)
9	Jerusalem West cave	speleothem	$\delta^{18}O$	35.15	31.78	700	168,714-present	Frumkin et al., (1999); Shah et al., (2013)
10	Soreq cave	speleothem	$\delta^{18}O$	35.03	31.45	400	30,031-present	Bar-Matthews et al., (2003); Shah et al., (2013)
11	Kuna Ba cave	speleothem	$\delta^{18}O$	45.64	35.16	660	3988-present	Sinha et al. (2019)
12	Lake Zeribar	lake sediments	$\delta^{18}O$	46.11	35.53	1300	20,746-108	Stevens et al., (2001); Roberts et al., (2008)
13	Lake Mirabad	lake sediments	$\delta^{18}O$	47.72	33.08	800	9338-55	Stevens et al., (2006); Roberts et al., (2008)
14	Gol-e-Zard cave	speleothem	$\delta^{18}O$	52	35.84	2535	4920–3770	Carolin et al., 2019(Carolin et al., 2019)
15	Hoti cave	speleothem	$\delta^{18}O$	57.35	23.08	800	9607-6026	Neff et al. (2001)
16	Qunf cave	speleothem	$\delta^{18}O$	54.18	17.1	650	10,558–2700, 1312-308 BP	Fleitmann et al., (2007); Shah et al., (2013)

63–65). The method assumes that the total probability of an archaeological event (site occupation phase in our case) within a given time span is 1, which indicates an absolute certainty that the site was in use in that time span. If we then divide by the length of the site's chronological range, we can represent the probability of existence for each temporal block (implicitly adopting a default uniform assumption). For instance, using time-steps of 200 years, a Middle Bronze Age site-phase ranging from 2000 to 1600 BC has an aoristic weight of 0.50 for each time-step (2000–1800, 1800–1600). In addition, to mitigate the discrepancy between long individual phases within typo-chronological schemes and likely shorter term durations of site occupations, we applied Monte Carlo methods to generate randomised start occupation periods for those sites with low-resolution information, assuming a mean length of occupation of 200 years within each cultural period (cf. Crema 2012, 450–451; Orton et al., 2017, 5–6; Palmisano et al., 2017, 63–64). The 200-year duration was used to correspond to the median duration of the cultural periods (or site-phases) of the settlements employed in this study and to offer a clear contrast for those periods having large time spans (e.g. 1000 years or more). The resulting probabilistic distributions (aoristic weights, randomised start dates) provide a robust dataset to compare with other archaeo-demographic proxies.

3.2. Creating SPD of calibrated radiocarbon dates

The SPD of calibrated radiocarbon dates is the result of counting up (summed in the manner of a histogram) the calibrated raw radiocarbon years of each organic sample, which are expressed in the form of probability statements with error ranges. The idea is that the more people living in a given region, the more garbage, the more organic materials, and the more radiocarbon collected, and dated (Rick 1987).

We used the R package *rcarbon* (version 1.4.1; see Bevan and Crema 2020 ; Crema and Bevan 2020) for generating and statistically assessing the SPDs of calibrated radiocarbon dates. We calibrated and summed individual radiocarbon dates within a broader temporal coverage than our study period, between 15,000 and 2000 cal. yr. BP, to avoid any edge effects. We reduced any bias of oversampling of specific chronological phases or events (for example, multiple dates being taken from a single floor layer) by aggregating uncalibrated radiocarbon dates within 50-year bins; dates with a gap greater than 50 years were assigned to a separate bin. We then calibrated the radiocarbon dates and pooled mean probabilities within the bins to have only one date distribution for each 50-year archaeological context (cf. Timpson et al., 2014). Hence, the probability distributions of 10,653 calibrated radiocarbon dates from 993 sites have been aggregated into 4873 (50-year) site bins and finally summed to produce SPDs for the Near East as a whole and for the seven sub-regions (Anatolia, Arabia, Cyprus, Iran, Levant, Mesopotamia, and South Caucasus). We opted to sum unnormalised distributions of calibrated radiocarbon dates as some recent work (Weninger et al., 2015; Bevan et al., 2017) has suggested that normalised dates create artificial peaks in the resulting SPDs due to the steepening portions of the radiocarbon calibration curve (we have used the IntCal20 curve; Reimer et al., 2020).

We compared the observed SPD of calibrated radiocarbon dates with two theoretical null models of demographic change to statistically determine if the inferred population fluctuations indicate meaningful departures from what may be expected by mere chance. Put simply, the observed SPD were compared with conditional random sets of hypothetical dates produced according to two theoretical null models of population growth (exponential and logistic). First, we fitted both an exponential and a logistic model of demographic growth to the observed data, and then back-calibrated new random samples (equal to the number of site-bins) drawn from the fitted model (Bevan and Crema 2020: modelTest). These hypothetical samples were then calibrated and their probability distributions summed to generate an expected SPD of the fitted null model. We repeated the same process 1000 times to provide a test of global goodness-of-fit and a 95% confidence envelope (in grey in the relevant figures). Departures of the observed SPD (solid black line in the figures) above and below the confidence envelope indicate respectively periods of increase (in red in the relevant figures) or decrease (in blue in the relevant figures) greater

than expected according to a null model of growth. Although both logistic and exponential models are theoretical abstractions not describing any empirically derived population growth, they are useful for assessing significant patterns in population fluctuations across time (Turchin 2001). The logistic model, based on the Malthusian assumption that population growth is limited by a maximum imposed by the carrying capacity of the environment, could fit a scenario characterised by a dramatic increase in population with the introduction of farming and a gradual demographic slowdown in the later periods as local resource limits are reached (Bevan et al., 2017; Palmisano et al., 2019). The exponential null model has the advantage of mimicking site loss through time and/or expected multi-millennial demographic trends (Shennan et al., 2013).

Finally, we assessed regional variation in population dynamics by performing a permutation test to assess to what degree the SPDs of each region depart from a null model representing the pan-regional demographic trends across the whole Near East (cf. Crema 2016; Bevan and Crema 2019: permTest). This technique shuffles the labels identifying from which region each bin comes and generates 1000 SPDs from which a 95% confidence envelope is derived. Deviations from the null model indicate periods in which the population increase (in red) or decline (in blue) of each region is greater than the pan-regional trend.

4. Results

4.1. Demographic trends inferred from SPDs of radiocarbon dates

We generated a normalised (black line) and unnormalised (in grey) SPD of calibrated radiocarbon dates (Fig. 2a) for the period from 14,000–2500 cal. yr. BP. Despite our preference for summing unnormalised calibrated dates, which avoids artificial spikes in the resulting SPDs, the two curves appear very similar, as shown by a high Pearson correlation coefficient ($r = 0.91$, p-value < 0.01). Given that most dates come from wood charcoal or unidentified material, we also produced an SPD of unnormalised radiocarbon dates from short-lived radiocarbon samples (e.g. bones, collagen, seeds, grains). The SPDs including all dates (Fig. 2a) and only short-lived dates (Fig. 2b) are highly correlated ($r = 0.95$, p-value $= 0.01$, Pearson) and the so-called old wood effect seems not to have significantly affected the resulting post-calibration probability densities. Fig. 2c and d shows the comparison of the SPD of unnormalised calibrated radiocarbon with logistic and exponential null models respectively. The observed SPDs (black solid line) show coincident positive (in red) and negative (in blue) deviations from the 95% confidence interval only from 5300 cal. yr. BP onwards (Fig. 2c and d). The inferred demographic trends show significant departures from the null model and on the basis of the global p-value (<0.01) we can say that the population did not grow neither logistically nor exponentially from the Late Pleistocene to the Late Holocene (14,000–2500 cal. yr. BP). The SPD of calibrated radiocarbon dates suggests that population increased prominently at around 12,700–12,600 cal. yr. BP, remained steady during the Younger Dryas stadial (~12,500–11,700), and saw significant growth at the beginning of the Holocene (~11,600–11,300 cal. yr. BP). Continuous growth of population occurred until 8500 cal. yr. BP. In the Middle Holocene (between 8500 and 5500 cal. yr. BP), the population was quite stable and was characterised by alternating periods of moderate increase and strong decline. The population increased strongly between 5300 and 4200 cal. yr. BP and peaked during 3200–2900 cal. yr. BP. The final decline in SPD after 2800 cal. yr. is likely not reflective of past population, but is rather due to the fact that researchers rely less on radiocarbon dating given the problem represented by the Hallstatt plateau, as explained above, and greater refinement in ceramic typologies.

Fig. 3 shows the regionally subdivided SPD of unnormalised radiocarbon dates compared against the pan-regional trend (grey envelope) described above. We examined to what degree regional demographic fluctuations depart from the pan-regional trends via a permutation test (cf. Crema et al., 2016). This technique also deals with issues resulting from the different sizes of the samples, as the grey envelopes of pan-regional trends produced are larger in those regions with fewer radiocarbon dates, reflecting greater uncertainty. All seven regions show significant departures from the pan-regional trend over the long-term (p-value < 0.01). The population level was quite low across the whole Near East during the Epipaleolithic, with the Levant and Mesopotamia showing significant positive departures from the pan-regional trend (Fig. 3d and e). In contrast, during the Holocene we have greater regional variation. Anatolia and the South Caucasus show similar demographic trends with a marked increase of population between 8000 and 7000 cal. yr. BP and during the Bronze Age (5000-3000 cal. Yr. BP), punctuated by a general decline in the Chalcolithic. The South Caucasus, unlike Anatolia, shows a significant positive departure from the pan-regional trend during the Late Bronze and Iron Ages (3500-2500 cal. yr. BP; Fig. 3b). The Levant and Cyprus show similar population patterns across the Holocene with some striking differences in particular periods. For instance, in Cyprus population departs positively from the global pattern during the Aceramic Neolithic (11,000–9500 cal. yr. BP) and the Late Bronze Age (Fig. 3c), while in the Levant we can see that population levels off significantly between 9000 and 7200 cal. yr. BP and reaches a peak in the Early Iron Age (3200-2800 cal. yr. BP, Fig. 3d). Mesopotamia shows positive deviations during the Pre-Pottery Neolithic (PPN), Neolithic and Early Bronze Age, while population declines noticeably in the later periods (Iron Age), likely related to a combination of a lack of excavations, an increase in ceramic typology accuracy and the Hallstatt plateau in the radiocarbon curve discussed above (Fig. 3e). Iran shows alternating patterns of population booms and busts across the whole Holocene (Fig. 3f). Finally, the Arabian Peninsula shows a significant departure from the pan-regional trend during the Neolithic (7400-6400 cal. yr. BP) and a marked demographic drop in the Bronze Age (Fig. 3g). However, in this area the available radiocarbon dates are patchy and, therefore, the inferred population dynamics should be regarded cautiously.

Pairwise Pearson's correlations between all regional SPDs have been calculated in order to assess how demographic patterns differed among the regions in three discrete sub-periods: 1) Late Pleistocene and Early Holocene (14,000–8326 cal. yr. BP, Table 3); 2) Middle Holocene (8326–4200 cal. yr. BP, Table 4); 3) Late Holocene (4200–2500 cal. yr. BP, Table 5). The results show similar demographic trends across the Near East in the Late Pleistocene-Early Holocene except for the South Caucasus (Table 3), increased regionalisation during the Middle Holocene (Table 4), and marked interregional differences in the Late Holocene (Table 5; see Fig. 4a).

4.2. Assessing population dynamics from multiple proxies: a standalone evaluation

Here, we compare the demographic trends for three areas where we have both site survey data and radiocarbon dates: Anatolia, Southern Levant and Upper Mesopotamia (Fig. 5). The archaeological settlement data derived proxies (raw count, total aggregated estimated size, aoristic weight, randomised start occupation dates) and the SPD of calibrated radiocarbon dates have been normalised on a scale from 0 to 1 in order to make them comparable. All proxies have been binned into 200-year time slices to correspond to the median site-phase lengths.

In Anatolia, we can see a correspondence between the sites

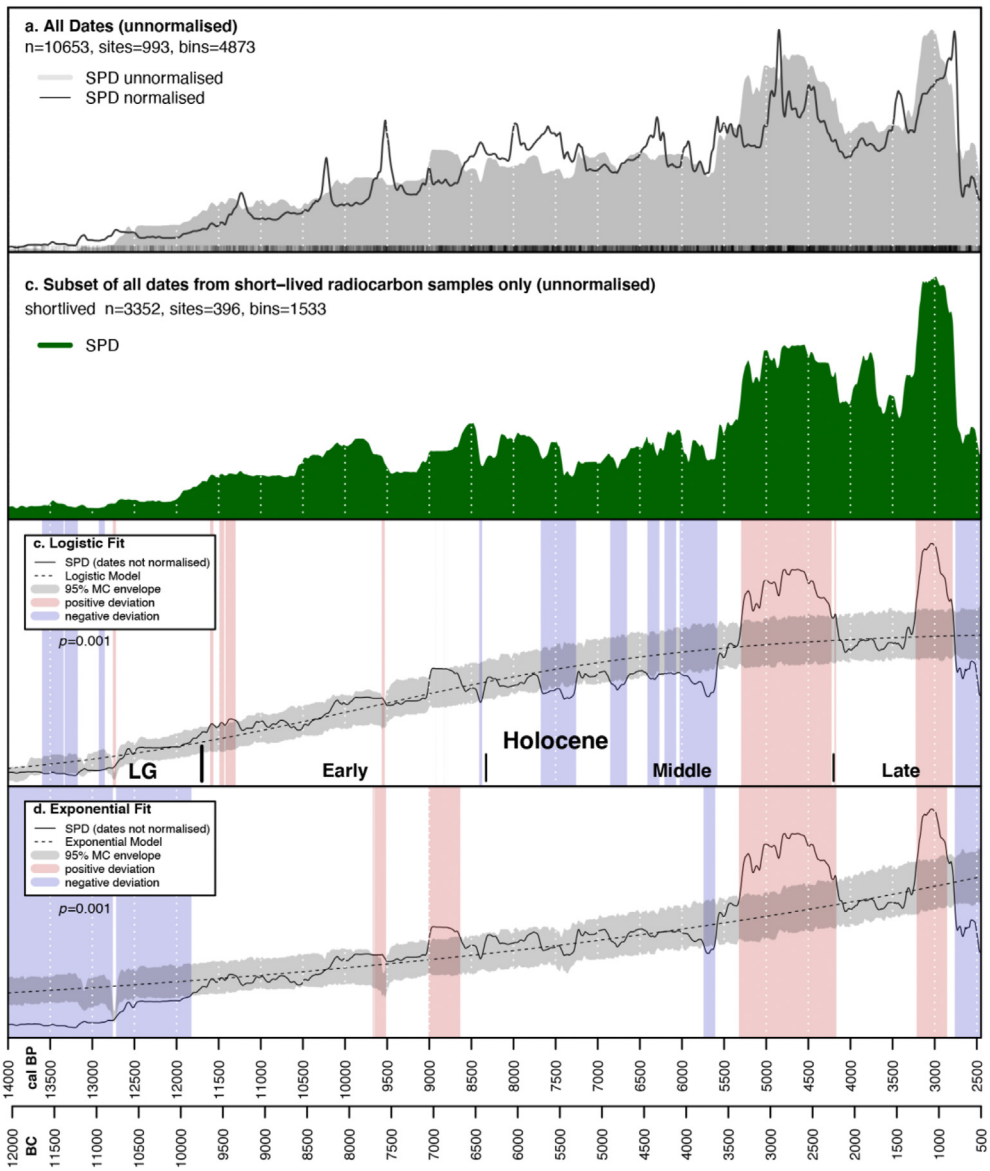

Fig. 2. a) Summed Probability Distribution (SPD) of normalised (black line) and unnormalised (in grey) calibrated radiocarbon dates; the bar-code like strip represents the median values of multiple calibrated radiocarbon bins; b) unnormalised SPD of short-lived radiocarbon dates; c) unnormalised SPD (solid line) vs. a fitted logistic and d) exponential null model (95% confidence grey envelope). Blue and red vertical bands indicate respectively chronological ranges within the observed SPD deviates negatively and positively from the null model. (For interpretation of the references to colour in this figure legend, the reader is referred to the Web version of this article.)

derived proxies and the SPD of radiocarbon dates (see Fig. 5a and Table 6). The correlation between the SPDs of radiocarbon dates and the other proxies is stronger between 10,000 and 4000 cal. yr. BP (Table 7). This is due to the fact that in the later periods the SPDs tend to underestimate the population as archaeologists rely more on ceramic-based typo-chronologies. However, the settlement data appear to be poorly correlated with the SPD of south-central Anatolia (Table 6). This issue is related to the fact that the SPD curve for central Anatolia is skewed by the disproportionately large number of dates from Çatalhöyük (282 out of 902), and by the fact that radiocarbon dates have not been published for several known Bronze and Iron Ages centres. In the Levant, the settlement derived proxies and the SPDs appear to be strongly correlated (Fig. 5b, Tables 8 and 9). The Early Bronze Age (5400–4000 BP) is over-represented in the SPD, and there is a major spike in the early part of the Iron Age (3300–2500 BP). Both of these can be interpreted as a result of biases in research intensity. The EBA saw the emergence of complex polities and as a result has received significant scholarly attention, while the interests of Biblical Archaeology in the Southern Levant have resulted in a large number of projects focused on this period. In Upper Mesopotamia, the settlement derived proxies and the SPD of radiocarbon dates are quite well correlated during the period between 8400 and 4000 cal. yr. BP (Fig. 5c; Tables 10 and 11). Fluctuations in the SPD during the Late Chalcolithic (6500–5000 cal. yr. BP) are not reflected in either of the settlement record proxies and as in the Southern Levant there is a peak in the Early Bronze Age which may in part reflect biases in research agendas. The settlement data in this region is especially poor for the Early Holocene, when the SPD suggests very high levels of population. Here unusual research interest in early farming communities is likely inflating the SPD, while surveys reliant on ceramics as key indicators of archaeological sites struggle to identify pre-pottery occupation. Conversely, from 4000 cal. yr. BP onwards the SPD depict a drastic drop in the population, while

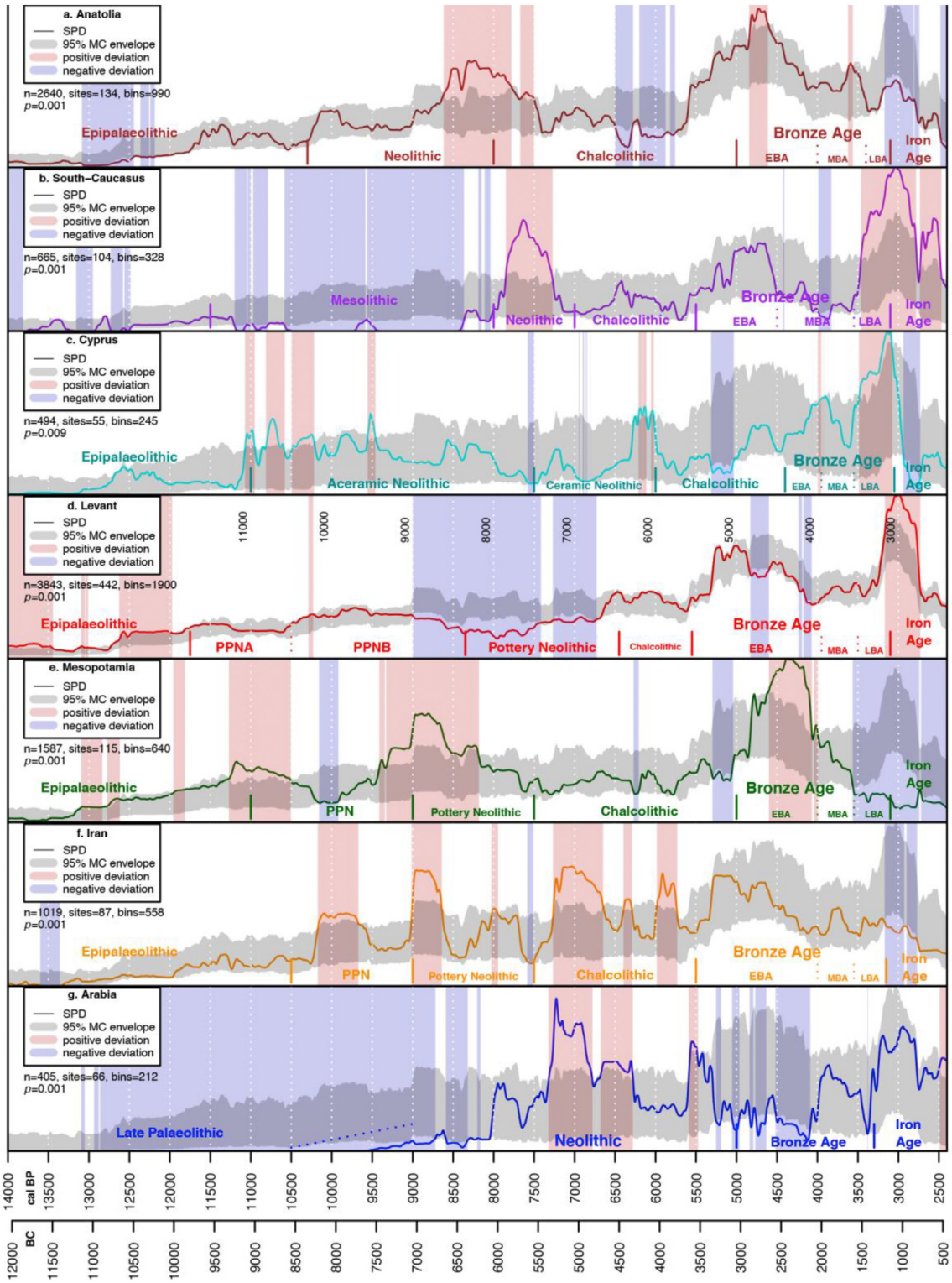

Fig. 3. Regional summed probability distributions (SPDs) of calibrated radiocarbon dates for a) Anatolia, b) South Caucasus, c) Cyprus, d) Levant, e) Mesopotamia, f) Iran, and (g) Arabia compared with a 95% Monte Carlo envelope of the pan-regional model produced via permutation of sub-regional dates.

surveys suggest a minor decline followed by a major increase. While the initial decline during the Late Bronze Age may be genuine, during the Iron Age surveys have identified large numbers of small rural sites, often at new locations away from the long-term occupations on settlement mounds (Wilkinson 2003). Very few of these have been subject to excavation and are therefore not captured by the SPD.

To summarise, the overall agreement between the radiocarbon SPD dates and the settlement-based proxies corroborates the use of the former as a quite good indicator for inferring past human population dynamics. However, it is important to stress that these proxies should be used complementarily and contextually to

Table 3
Pearson Correlation Coefficient r-value matrix in the Late Pleistocene and Early Holocene between the regional SPDs (14,000–8326 cal. yr. BP). Strong correlations are indicated by bold numbers. *p-value < 0.05

	Anatolia	South Caucasus	Cyprus	Levant	Mesopotamia	Iran	Arabia
Anatolia	1.00						
South Caucasus	−0.15	1.00					
Cyprus	***0.60**	−0.25	1.00				
Levant	***0.67**	−0.14	***0.71**	1.00			
Mesopotamia	***0.72**	−0.16	*0.47	***0.58**	1.00		
Iran	***0.71**	−0.31	***0.51**	***0.73**	***0.71**	1.00	
Arabia	***0.65**	−0.31	0.22	0.32	***0.77**	***0.59**	**1.00**

Table 4
Pearson Correlation Coefficient r-value matrix in the Middle Holocene between the regional SPDs (8326-4200 cal. yr. BP). Strong correlations are indicated by bold numbers. *p-value < 0.05

	Anatolia	South Caucasus	Cyprus	Levant	Mesopotamia	Iran	Arabia
Anatolia	1.00						
South Caucasus	*0.39	1.00					
Cyprus	0.29	−0.01	1.00				
Levant	*0.48	0.23	*0.41	1.00			
Mesopotamia	***0.68**	0.13	***0.51**	*0.47	1.00		
Iran	0.20	−0.19	−0.08	*0.39	0.03	1.00	
Arabia	***-0.47**	−0.28	−0.35	−0.26	*-0.42	0.30	1.00

Table 5
Pearson Correlation Coefficient r-value matrix in the Late Holocene between the regional SPDs (4200-2500 cal. yr. BP). Strong correlations are indicated by bold numbers. *p-value < 0.05.

	Anatolia	South Caucasus	Cyprus	Levant	Mesopotamia	Iran	Arabia
Anatolia	1.00						
South Caucasus	*-0.38	1.00					
Cyprus	*0.33	0.22	1.00				
Levant	0.08	***0.75**	0.10	1.00			
Mesopotamia	*0.43	***-0.68**	0.03	***-0.50**	1.00		
Iran	*0.46	−0.16	*0.49	0.06	0.23	1.00	
Arabia	−0.15	***0.59**	−0.06	***0.76**	***-0.64**	−0.06	1.00

provide a more complete picture. Broadly speaking, the curves inferred from survey data tend to minimise the population levels in the earlier periods while the SPDs of radiocarbon dates overestimate population in prehistoric periods. Survey projects tend to rely on pottery for dating, and therefore prehistoric sites with no pottery or very long lived types are underrepresented. Excavators at such sites tend to take more radiocarbon dates than those working in later periods. A clear caveat in the SPD for Anatolia and Upper Mesopotamia is that they fail to show the demographic booms inferred from increased site counts and total settled area related to the Hittite (ca. 3600-3200 cal. yr. BP; Fig. 5a) and Neo-Assyrian (ca. 2900-2600 cal. yr. BP) Empires (Fig. 5c). In the discussion section below, we interpret our wider results in the light of these limitations.

4.3. A reconstruction of climate during the Late Pleistocene and the Holocene

The available palaeoclimatic records indicate that after a long period of cooling in the Late Pleistocene (the Younger Dryas: ~12,700–11,700 cal. yr. BP), which reversed the gradual climatic warming of the Bølling-Allerød interstadial (~14,700–12,700 cal. yr. BP), the onset of the Holocene was characterised by a switch towards warmer and wetter climatic conditions (Grootes and Stuiver 1997; Roberts et al., 2008; Dean et al., 2015). The transition from the Late Pleistocene to the Early Holocene seems to have occurred abruptly, as suggested by some records from Anatolia (see Fig. 6: 3–4, 6), the Levant (Fig. 6:7–10), and the Iranian plateau (Fig. 6:12). The $\delta^{18}O$ values of the Sofular and Karaca caves are in contrast with all the other records in this study, showing a gradual decrease of precipitation since the beginning of the Holocene (Fig.6; 2). However, the records from these two caves seem to reflect change in the $\delta^{18}O$ values of the Black Sea, the main source of moisture for these sites, rather than variation in rainfall (Fleitmann et al., 2009; Göktürk et al., 2011). The Holocene was characterised by wetter conditions between 10,000 and 7000 cal. yr. BP with peaks in rainfall at ~8500 and 7500 cal. yr. BP (Fig. 6; Burstyn 2019; Jones et al., 2019). After 7000 cal. yr. BP there is a progressive shift towards more arid conditions in most of the records. Although the general trends described above are quite homogeneous across the whole Near East, the records from Hoti and Qunf caves, both located in Oman on the Eastern side of the Arabian peninsula (Fig. 6: 15–16), show a decrease in precipitation one millennium later, at ~ 6000 cal. yr. BP, due to the strength of the Indian Ocean monsoon (Neff et al., 2001; Fletimann et al., 2007). The Late Holocene was generally a dry period characterised by pronounced sub-centennials fluctuations of dry episodes (4300–3800 cal. yr. BP; 3200-2900 cal. yr. BP) punctuated by a period of increasing precipitation (~3800–3200 cal. yr. BP; Grant et al., 2012; Burstyn et al., 2019).

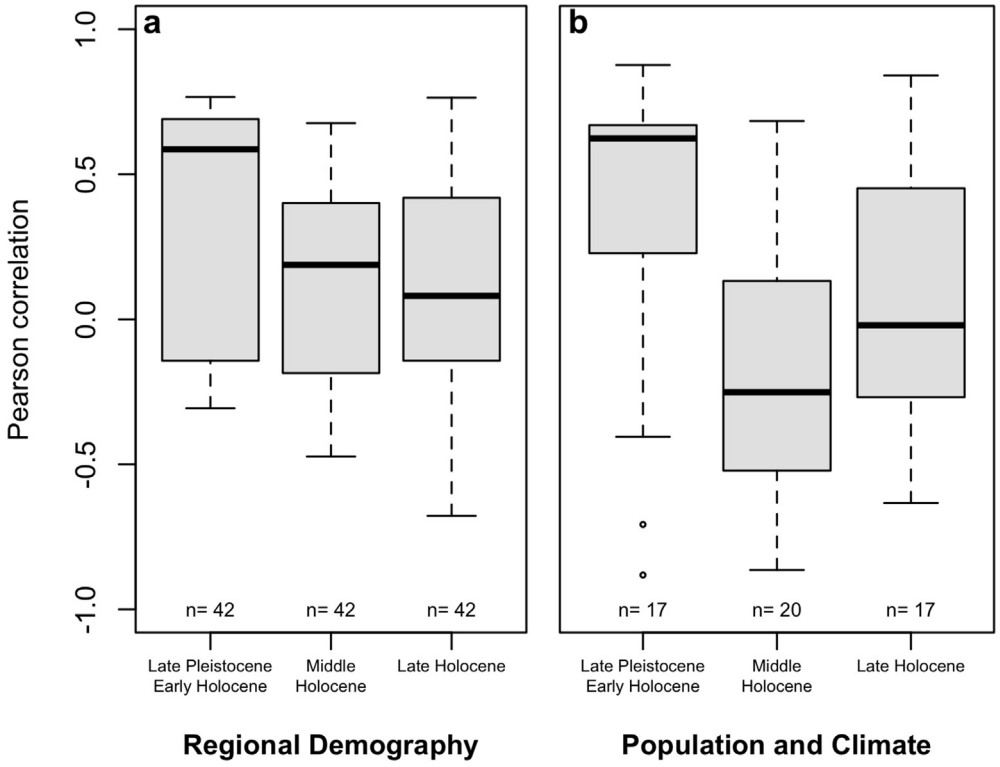

Fig. 4. Box-plots showing the pairwise Pearson correlation values between all regional SPDs (a) and between population and climatic trends (b); n = number of correlations performed.

At a shorter timescale, the Holocene was characterised by multi-centennial and multi-decadal dry and wet episodes that caused abrupt changes in the longer millennial climatic trends. In this study, we will focus on five major RCCs (the 10.2 k, 9.2 k, 8.2 k, 4.2 k, and 3.2 k cal. yr. BP 'events') that have been the focus of academic debate addressing the human responses to climate change (see Table 12). The 10.2 k cal. yr. BP event took place between 10,200 and 9800 cal. tr. BP and is visible in some palaeoclimatic records from Anatolia (Fig. 6:1–2, 5–6) and the Levant (Fig. 6: 7–8; Table 12). The 9.2 k cal. yr. BP event seems to have a relatively small impact in the Near East as the only records showing a substantial decrease in precipitation are Lake Gölhisar and Sofular cave in Anatolia (Fig. 6:1–2) and the Hoti and Qunf caves in Oman (Fig. 6: 15–16; Table 12; Fleitmann et al., 2015). The 8.2 k cal. yr. BP event took place between 8250 and 8000 cal. yr. BP and was characterised by a decrease in global temperatures and snow accumulation rate (Thomas et al., 2007; Cheng et al., 2009). This event is visible in most of the records used in this study, although Lake Hula in Northern Israel (Fig. 6:8) and Lake Mirabad in Iran (Fig. 6:13) saw an increase in rainfall (Table 12). The 4.2 cal. yr. BP was a cold and dry episode between 4300 and 3800 cal. yr. BP, which marked the transition to the Late Holocene and a shift towards more arid climatic conditions. Several scholars have argued that it caused considerable environmental stress affecting Near Eastern societies (Weiss 2016; Kaniewski et al., 2018; Bini et al., 2019). This abrupt climatic shift is evident in almost all records and seems to indicate a drying phase across the whole Near East (Fig. 6; Table 12). The final significant RCC occurred between 3200 and 2900 cal. yr. BP and is in line with the longer multi-millennial drying trend characterising the Late Holocene (Fig. 6; Kaniewski et al., 2015 and 2019). The high-resolution climate records such as Sofular Cave in Turkey, Jeita Cave in Lebanon, Kuna Ba cave in northern Iraq, and the Qunf cave in Oman indicate that this climatic event was characterised by pronounced multi-decadal fluctuations of wet and dry episodes (Fig. 6: 2, 7, 14, and 16; Kuzucuoğlu, 2009; Shah et al., 2013; Cheng et al., 2015.)

4.4. Comparing demographic and climatic trends over long and short timescales: a regional analysis

The SPDs of calibrated radiocarbon dates and the z-scores of those palaeoclimate records with a sufficiently fine resolution have been binned into 50-year time slices. The use of a 50-year time window is only possible for those palaeoclimate records having a mean sampling interval lower than 50-years across the whole chronological scope (Fig. 6:2,7,11,14–16).

The palaeoclimate records with a coarser chronological resolution and with dates greater than 50 years from one to another have been binned into 100-year (Fig. 6: 4), 300-year (Fig. 6:1,3,5,6,8) 400-year (Fig. 6:13), 500-year (Fig. 6:10,12) and 600-year (Fig. 6:9) time slices. The SPD were binned into coarser time slices when compared with these palaeoclimate records. For those palaeoclimatic records with a finer resolution and a long chronological span, we have calculated a 500-year time window Pearson correlation with ten 50-year bins in each time window (Fig. 6: 2,7, and 16). The advantage of this approach is to identify periods of correspondence and divergence between human population size and palaeoclimate records over shorter periods from the Late Pleistocene to the late Holocene (14,000–2500 cal. yr. BP). We then calculated Pearson correlations with maximum and minimum values ranging respectively between 1 and -1 in order to assess if the population dynamics are positively or negatively correlated with hydro-climatic trends.

In Anatolia, the long-term demographic and climatic trends show diverging patterns, as shown by strong negative Pearson correlation values ranging between −0.39 and −0.74, with the only

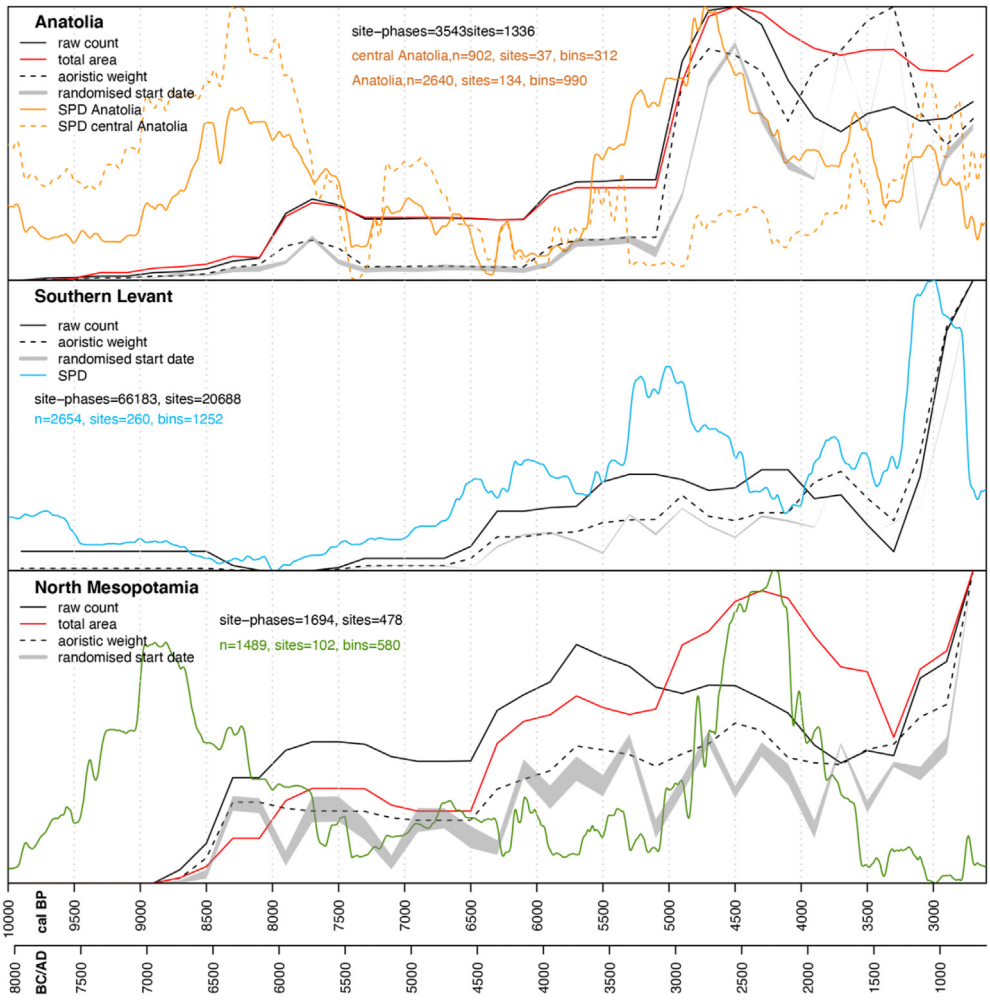

Fig. 5. Normalised archaeo-demographic proxies for a) Anatolia, b) Southern Levant, and c) Upper Mesopotamia.

Table 6
Pearson Correlation Coefficient r-value matrix between the demographic proxies of Anatolia between 10,000 and 2600 cal. yr. BP). Strong correlations are indicated by bold numbers. *p-value < 0.05

	Count	Area	Aoristic weight	Random	SPD Anatolia	SPD Central Anatolia
Count	1.00					
Area	**0.97***	1.00				
Aoristic weight	**0.89***	**0.95***	**1.00**			
Random	**0.84***	**0.89***	**0.93***	1.00		
SPD Anatolia	**0.61***	**0.54***	**0.55***	**0.49***	1.00	
SPD Central Anatolia	−0.40*	−0.33	−0.24	−0.22	0.09	1.00

Table 7
Pearson Correlation Coefficient r-value matrix between the demographic proxies of Anatolia between 10,000 and 4000 cal. yr. BP. Strong correlations are indicated by bold numbers. *p-value < 0.05

	Count	Area	Aoristic weight	Random	SPD Anatolia	SPD Central Anatolia
Count	1.00					
Area	**0.99***	1.00				
Aoristic weight	**0.97***	**0.96***	1.00			
Random	**0.94***	**0.94***	**0.96***	1.00		
SPD Anatolia	**0.67***	**0.65***	**0.73***	**0.70***	1.00	
SPD Central Anatolia	**−0.49***	**−0.47***	−0.35	−0.31	0.10	1.00

Table 8
Pearson Correlation Coefficient r-value matrix between the demographic proxies of southern Levant between 10,000 and 2600 cal. yr. BP. Strong correlations are indicated by bold numbers. *p-value < 0.05

	Count	Aoristic weight	Random	SPD
Count	1.00			
Aoristic weight	**0.95***	1.00		
Random	**0.93***	**0.97***	1.00	
SPD	**0.69***	**0.69***	**0.57***	1.00

Table 9
Pearson Correlation Coefficient r-value matrix between the demographic proxies of southern Levant between 10,000 and 4000 cal. yr. BP. Strong correlations are indicated by bold numbers. *p-value < 0.05

	Count	Aoristic weight	Random	SPD
Count	1.00			
Aoristic weight	**0.97***	1.00		
Random	**0.93***	**0.96***	1.00	
SPD	**0.85***	**0.87***	**0.82***	1.00

Table 10
Pearson Correlation Coefficient r-value matrix between the demographic proxies of Upper Mesopotamia between 8400 and 2600 cal. yr. BP. Strong correlations are indicated by bold numbers. *p-value < 0.05

	Count	Area	Aoristic weight	Random	SPD
Count	1.00				
Area	**0.67***	1.00			
Aoristic weight	**0.81***	**0.80***	1.00		
Random	**0.70***	**0.64***	**0.88***	1.00	
SPD	−0.10	0.38*	0.01	0.02	1.00

Table 11
Pearson Correlation Coefficient r-value matrix between the demographic proxies of Upper Mesopotamia between 8400 and 4000 cal. yr. BP. Strong correlations are indicated by bold numbers. *p-value < 0.05

	Count	Area	Aoristic weight	Random	SPD
Count	1.00				
Area	**0.75***	1.00			
Aoristic weight	**0.85***	**0.92***	1.00		
Random	**0.62***	**0.69***	**0.76***	1.00	
SPD	0.06	**0.63***	**0.54***	0.46*	1.00

exception being Lake Van (r = 0.58, p-value <0.01). This is not surprising given that the population constantly and incrementally increases from the onset of the Holocene, while most of the palaeoclimatic records show a slow and gradual multi-millennial trend towards more arid conditions (Fig. 7). However, on a short-time scale, we can see that the demographic rise in the Epipalaeolithic and Early Neolithic coincided with a wetter climate at the beginning of the Holocene, as shown by the correlation value with the shorter duration dataset from Dim cave (r = 0.67, p-value <0.01). The significant increase in the population occurring between 8500 and 8000 cal. yr. BP seems to correspond with wetter conditions detectable in some records (Fig. 7: 1,5–6), while the decline during the Chalcolithic shows a good correspondence with a climatic drying phase after 7500 cal. yr. BP visible in all records except Lake Gölhisar. The population increased again between 5300 and 4400 cal. yr. BP despite a general arid trend and seems to have been negatively affected by the RCCs at 4.2 and 3.2 cal. yr. BP. Although to a minor degree for the total area of the sites, these two events are also present in the archaeological settlement data derived proxies (Fig. 5a).

Given the lack of available palaeoclimatic records in the South Caucasus, we compared the SPD against the nearest climatic records in our dataset, such as Karaca cave and Lake Van (Fig. 8). The lack of data does not allow for a direct comparison between demographic and climatic trends for the earlier periods. The increases in population during the Neolithic and the Early Bronze Age (EBA), interspersed by a substantial decline during the Chalcolithic, seem to correspond with two relatively wet periods separated by a drying climate between 7000 and 5600 cal. yr. BP. The population declined significantly in coincidence with the RCC at 4.2 cal. yr. BP and peaked dramatically during the Late Bronze age and Iron Age despite arid conditions.

As for the South Caucasus, we compared the SPD of radiocarbon dates from Cyprus with the closest palaeoclimatic records on the Levantine (Jeita Cave and Lake Hula) and Anatolian (Dim cave) coasts. An increase in the population and wetter climatic conditions during the Early Holocene appears synchronous, as suggested by strong Pearson correlation values between the SPD with the climatic trends provided by Dim cave (r = 0.67, p-value<0.01) and Jeita cave (Fig. 9). The 500-year moving window approach seems to identify a sort of sinusoidal cycle of alternating strong and negative correlations between demographic and climatic trends during the Middle Holocene. In the Late Holocene, the population grew substantially and peaked during the Late Bronze Age (3500-3000 cal. yr. BP) despite drier climatic conditions. However, the SPD curve and the climate patterns from Jeita cave are highly correlated between 3500 and 2500 cal. yr. BP (Fig. 9).

In the Levant, the population began to increase during the Epipalaeolithic, and a demographic bulge occurred in concordance with wetter climatic conditions between 10,500 and 9500 (Fig. 10). The initial demographic boom was followed by a decline in population during the Pottery Neolithic (ca. 8500-6500 cal. yr. BP), perhaps due to an overall climatic drying trend. The population peaked during the Early Bronze Age despite a drying of the climate and then declined markedly between 4200 and 3200 cal. yr. BP, a period characterised by pronounced sub-centennial dry-wet episodes superimposed onto an overall millennial drying trend. However, the population reached a peak in the Iron Age during a period of increasingly arid climatic conditions (Fig. 10).

In Mesopotamia, the population saw a first substantial growth in coincidence with ameliorated climatic conditions after the onset of the Holocene and boomed significantly between 9300 and 8300, when a peak in rainfall was reached (Fig. 11). A climatic drying trend between 8000 and 5000 seems to correlate with a fall in the population. Population peaked during the Early Bronze Age despite an even more arid climate. While a drop in population at the end of the Early Bronze Age could be related to the 4.2 k cal. yr. BP event, and the following decline during the Late Bronze Age is also confirmed by several studies using archaeological survey data (e.g. Ur 2013; Lawrence et al., 2017), very low demographic levels in the Iron Age are unrealistic and most likely due to a lack of a systematic collection of radiocarbon samples for this period. In fact, as indicated by the northern Mesopotamia settlements data (Fig. 5c), population started increasing and boomed during the Assyrian Empire.

In Iran we have a gradual increase in the population at the same time as wetter climatic conditions with the onset of the Holocene (Fig. 12). The significant booms and busts of the population during the Pottery Neolithic and Chalcolithic seem to be correlated with the climatic fluctuations inferred from the Lakes Zeribar and Mirabad. The time-series of the SPD curve and these two palaeoclimatic records are slightly offset because Lake Zeribar and Lake Mirabad have a mean sample interval greater than 170 years and were dated with conventional radiocarbon rather than with AMS techniques, meaning they are likely to be less accurate. In the Early Bronze Age, the population peaked again despite a shift towards

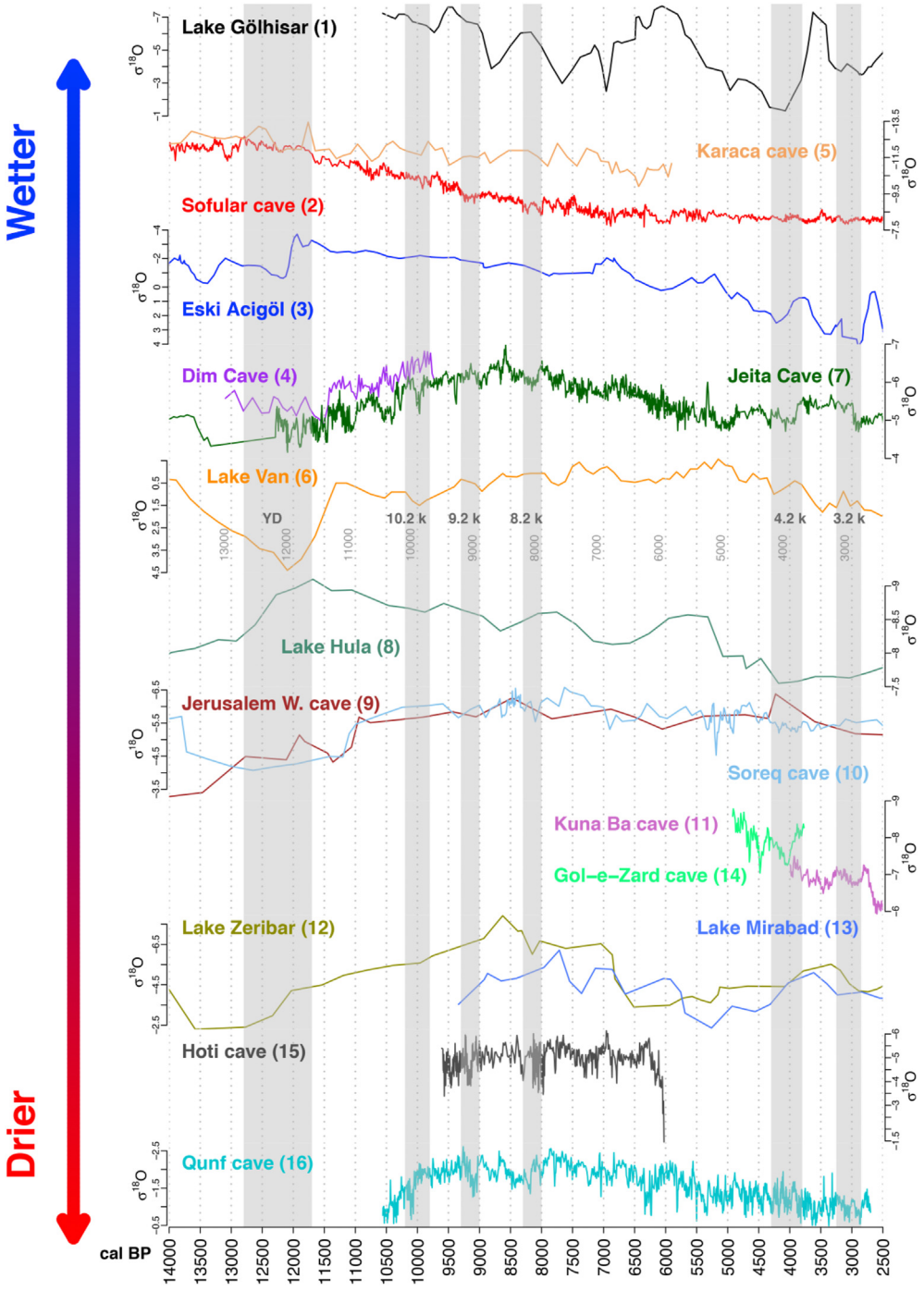

Fig. 6. Selected palaeoclimate proxies from the Middle East. The grey vertical bands indicate the Younger Dryas (YD), 10.2, 9.2, 8.2, 4.2 and 3.2 k yr. BP events.

arid conditions and then declined around the time of the 4.2 k cal. yr. BP event. Again, just as in Mesopotamia, the lower level of SPD curve during the Late Bronze and Iron Ages are likely due to research biases and do not represent past realities.

We do not have radiocarbon dates from the Arabian Peninsula for the earlier periods and, therefore, we cannot assess how the population responded to better climatic condition during the transition from the Late Pleistocene to the Early Holocene. We see that population grew substantially in the Neolithic, when the climate is relatively wet, and then declined in concomitance with a drying period from 6000 cal. yr. BP onwards (see Petraglia et al., 2020, Fig. 13). The population increased again in the Bronze Age and reached a peak in the Iron Age despite arid climate conditions.

The box-plots of all the Pearson correlation values show that population dynamics were positively correlated with climatic trends during the Late Pleistocene/Early Holocene (median = 0.65) while they decouple during the Middle and Late Holocene (Fig. 4b). It is important to stress that the correlation values could be even more negative during the Late Holocene given that in some regions the SPD of radiocarbon dates tend to depict unrealistic low population levels in the later periods (from ~3500 cal. yr. BP) when climate trends are towards more arid conditions. In fact, the site-

Table 12
Table showing the occurrence of the RCC in the paleoclimate records used in the present study.

Map no.	Site name	10. 2 k	9.2 k	8.2 k	4.2 k	3.2 k	Region
1	Lake Gölhisar	Yes	Yes	Yes	Yes	Yes	Anatolia
2	Sofular cave	Yes	Yes	Yes	Yes	Yes	Anatolia
3	Eski Acıgöl	/	/	Yes	Yes	Yes	Anatolia
4	Dim cave	/	/	Yes	Yes	Yes	Anatolia
5	Karaca cave	Yes	/	Yes	Yes	Yes	Anatolia
6	Lake Van	Yes	/	/	Yes	Yes	Anatolia
7	Jeita cave	Yes	/	Yes	Yes	Yes	Levant
8	Lake Hula	Yes	/	/	Yes	Yes	Levant
9	Jerusalem West cave	/	/	Yes	Yes	Yes	Levant
10	Soreq cave	/	/	Yes	Yes	Yes	Levant
11	Kuna Ba cave	/	/	/	Yes	Yes	Mesopotamia
12	Lake Zeribar	/	/	Yes	/	Yes	Iran
13	Lake Mirabad	/	/	/	/	Yes	Iran
14	Gol-e-Zard cave	/	/	/	Yes	Yes	Iran
15	Hoti cave	/	Yes	Yes	Yes	/	Arabia
16	Qunf cave	/	Yes	Yes	Yes	Yes	Arabia

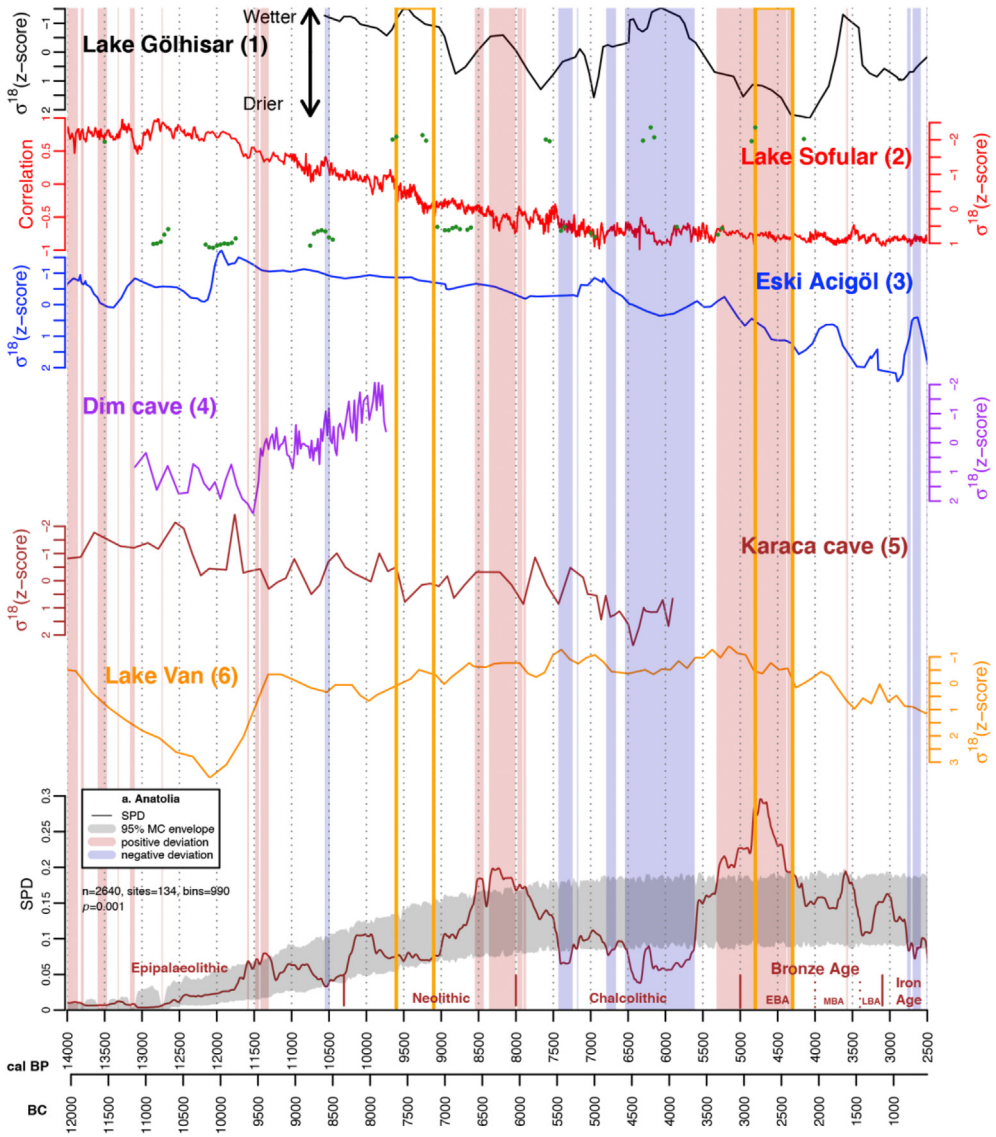

Fig. 7. SPD of unnormalised calibrated radiocarbon dates for Anatolia vs. a logistic null model (95% confidence grey envelope) compared with palaeoclimate records. Blue and red vertical bands indicate respectively chronological ranges within the observed SPD deviates negatively and positively from the null model. The green dots represent significant (p-value < 0.05) positive or negative Pearson's correlations (r) values ranging from +1 to −1 by using a 500-year-time moving window. The orange rectangle represents two examples of 500-year-time moving window (between 9600 and 9100 and 4800-4300 cal. yr. BP) in which the SPD of calibrated radiocarbon dates is significantly positively correlated with the climatic trends from Lake Sofular. (For interpretation of the references to colour in this figure legend, the reader is referred to the Web version of this article.)

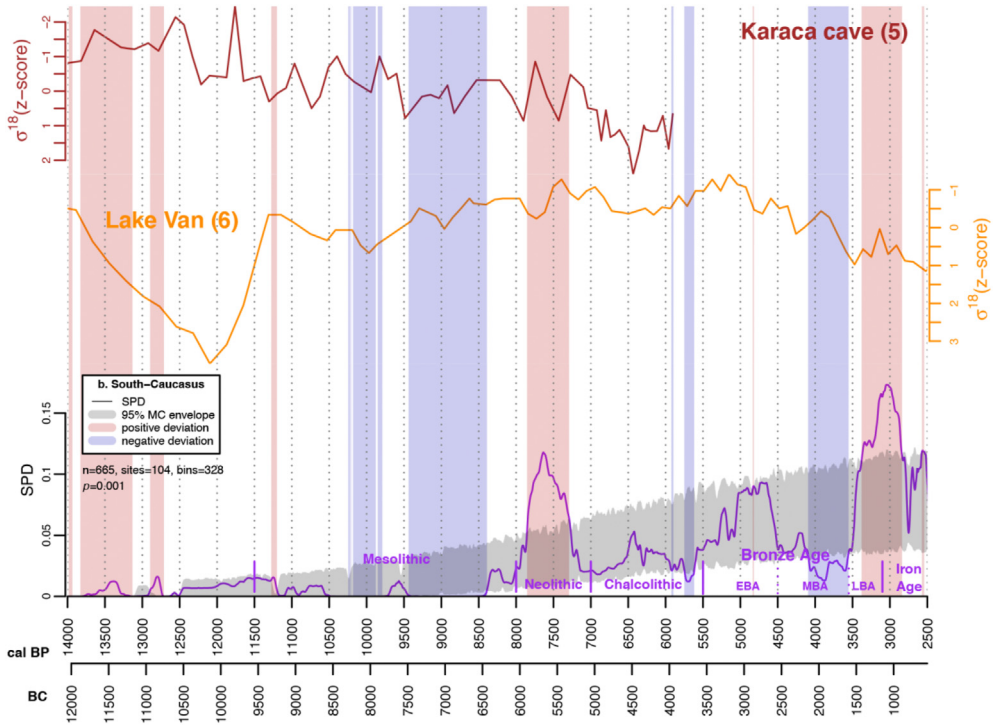

Fig. 8. SPD of unnormalised calibrated radiocarbon dates for South Caucasus vs. a logistic null model (95% confidence grey envelope) compared with palaeoclimate records Karaca Cave and Lake Van. Blue and red vertical bands indicate respectively chronological ranges within the observed SPD deviates negatively and positively from the null model. (For interpretation of the references to colour in this figure legend, the reader is referred to the Web version of this article.)

derived proxies from South-central Anatolia, Southern Levant and Upper Mesopotamia show higher population levels when compared to the SPDs of radiocarbon dates during the Late Holocene (Fig. 5). Thus, rather than a single step change between the Early Holocene and the Middle and Late Holocene, we would argue that from the second half of the Middle Holocene onwards we see an ongoing decrease in correlation between demographic and climate proxies.

5. Discussion

In this section, we illustrate more comprehensively where and when correlations between population dynamics and climatic trends occurred and describe how socio-ecological trajectories varied across the Near East from the Early to the Late Holocene. We are aware that the spatial and chronological scope of this work does not allow us to disentangle all the possible causal linkages between human-climate interactions, and caution is needed when constructing narratives of this kind. Our intention is to offer a first systematic assessment through the rigorous analysis of archaeological and climatic evidence. As stated above, our underlying assumption is that, all other factors remaining constant, increased aridity leads to population decline, and conversely that increased humidity supports population increase. Where these correlations are not present, or the magnitude of population change differs from that which we might expect given the magnitude of climate change, other factors may be involved. These include adaptive strategies such as social transformation and technological change, rapid declines in population and the complexity of social organisation, or migration. We should also remember that human groups are complex systems subject to endogenous change which may be unrelated to climate. We interpret our datasets within this framework.

5.1. Late Pleistocene and the Early Holocene (14,000–8326 cal. yr. BP)

The Late Pleistocene was characterised by the Bølling–Allerød interstadial, an abrupt warm and moist period (between 14,700 and 12,700) followed by a drying and cold climate during the Younger Dryas (ca. 12,700–11,700). The climate instability of the Late Pleistocene ended with the onset of the Holocene (ca. 11,700 cal. yr. BP), an overall thermally stable period characterised by higher average temperatures and wetter climatic conditions, which fostered radical environmental changes such as the growth of woodland vegetation, the retreat of permanent snowlines, and sea level rise (Lotter 2003; Roberts et al., 2008; Dean et al., 2015). Recent work has demonstrated that the domestication of cereal and legumes may have taken 2000–3000 years (Fuller et al., 2012; Asouti and Fuller 2012), and the climatic stability of the Holocene likely facilitated the establishment of farming. It is unlikely that such a long-term process could have occurred during the Late Pleistocene, a period characterised by pronounced climatic oscillations (Richerson et al., 2001). Put simply, the new multi-millennial moist climatic regime of the Early Holocene could have provided favourable conditions for the full domestication of crops, increasing sedentism and population growth (Richerson et al., 2001; Weninger 2017; Shennan 2018, 29–30, 37–38).

However, the Late Pleistocene-Early Holocene transition shows a more complex scenario with different regionalised climatic patterns. Several spatial climatic models in recent work by Roberts et al. (2018: Fig. 9) suggest that, despite a general drying phase across the Near East, favourable climatic conditions could have existed in the Fertile Crescent during the Younger Dryas (ca. 12,700–11,700 cal. yr. BP). As a consequence, unlike other Near Eastern regions, the Fertile Crescent experienced a stable climatic regime and could have acted as a refugia for plant and animal

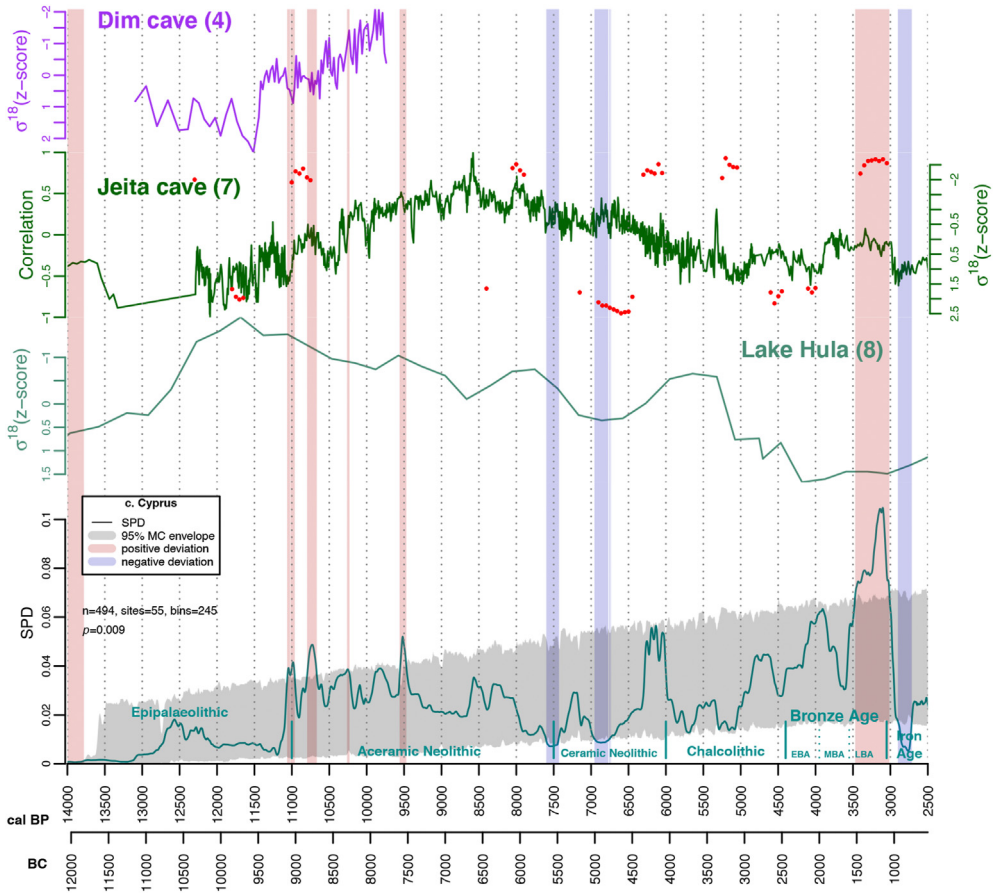

Fig. 9. SPD of unnormalised calibrated radiocarbon dates for Cyprus vs. a logistic null model (95% confidence grey envelope) compared with palaeoclimate records. Blue and red vertical bands indicate respectively chronological ranges within the observed SPD deviates negatively and positively from the null model. The red dots represent significant (p-value < 0.05) positive or negative Pearson's correlations (r) values ranging from +1 to −1 by using a 500-year-time moving window. (For interpretation of the references to colour in this figure legend, the reader is referred to the Web version of this article.)

resources and local human populations. This phenomenon may be visible in the SPDs of calibrated radiocarbon dates, where a rapid and continuous population growth occurred between 13,000 and 11,000 only in the Levant and Mesopotamia (Fig. 3: d-e; Figs. 10–11). In the other regions, the population level was quite flat and in Anatolia lied below the confidence envelope of the pan-regional trend (Fig. 3: a). With the onset of the Holocene, ameliorated climatic conditions and the demic spread of farming favoured population growth across the whole Near East. In Anatolia, a first substantial growth occurred in correspondence with the earliest evidence of sedentism and farming in south-central Anatolia at around 10,300 cal. yr. BP, as shown by the earliest archaeological levels from Boncuklu (Baird et al., 2012) and Aşıklı Höyük (Stiner 2014). A more dramatic increase in the population occurred between 8500 and 8000 cal. yr. BP when the whole of Anatolia was fully neolithicised (Brami 2015, Fig. 7). Both the Levant and Mesopotamia seem to have a static or declining population immediately after 11,000 cal. yr. BP, with some regional differences. The Levant experienced further population growth between 10,500 and 9500, after which followed a gradual decline (Fig. 10). In Upper Mesopotamia, a drastic decline of the population between 10,200 and 9800 cal. yr. BP was likely due to the 10.2 cal. yr. BP event that caused rapid cooling and drying, negatively affecting plant and animal biomass and the local incipient agrarian communities (Borrell et al., 2015, Fig. 11). However, the population started increasing again after the cooling event and boomed during the Pottery Neolithic between 9300 and 8200 cal. yr. BP, when permanent villages started spreading into fertile plains and along major rivers (Bader 1993; Campbell 2012; 421–422). This dramatic increase in population occurred simultaneously with the wettest climatic conditions across the whole Holocene (Fig. 11). A dramatic increase of population in Cyprus occurred with the onset of the Aceramic Neolithic at 11,000 cal. yr. BP and continued until 9500 cal. yr. BP (Fig. 9). This increase of population is perhaps related to several colonising events, where farmer-herder communities from the Levantine coast settled on the island (Peltenburg 2004; Simmons 2011). In Iran, a first increase in the population occurred during the Pre-Pottery Neolithic (PPN) with the earliest sedentary sites (e.g. Ganji Dareh, Asiab, Sarab) and in the first half of the ninth millennium BP when the communities on the Iranian plateau and highlands adopted a fully Neolithic lifestyle (Hole 1987; Zeder 2005; Helwing 2012, Fig. 12).

To summarise, after a climatic advantage to populations in regions such as the Levant and the Fertile Crescent during the Younger Dryas stadial, the onset of the Holocene brought an overall increase in temperature and rainfall across the whole Near East and facilitated the adoption of a sedentary lifestyle and demographic growth. The demic spread of the Neolithic package from the Levant at the beginning of the Holocene (~12,000 cal. yr. BP) to the South Caucasus by ~8000 cal. yr. BP (Fig. 3; cf. Bellwood 2013, 129–135) seems to have prompted a chronologically variable first substantial increase in population across different regions. In particular, population started growing during the Aceramic Neolithic and more markedly during the Pottery Neolithic (Fig. 3). On a multi-

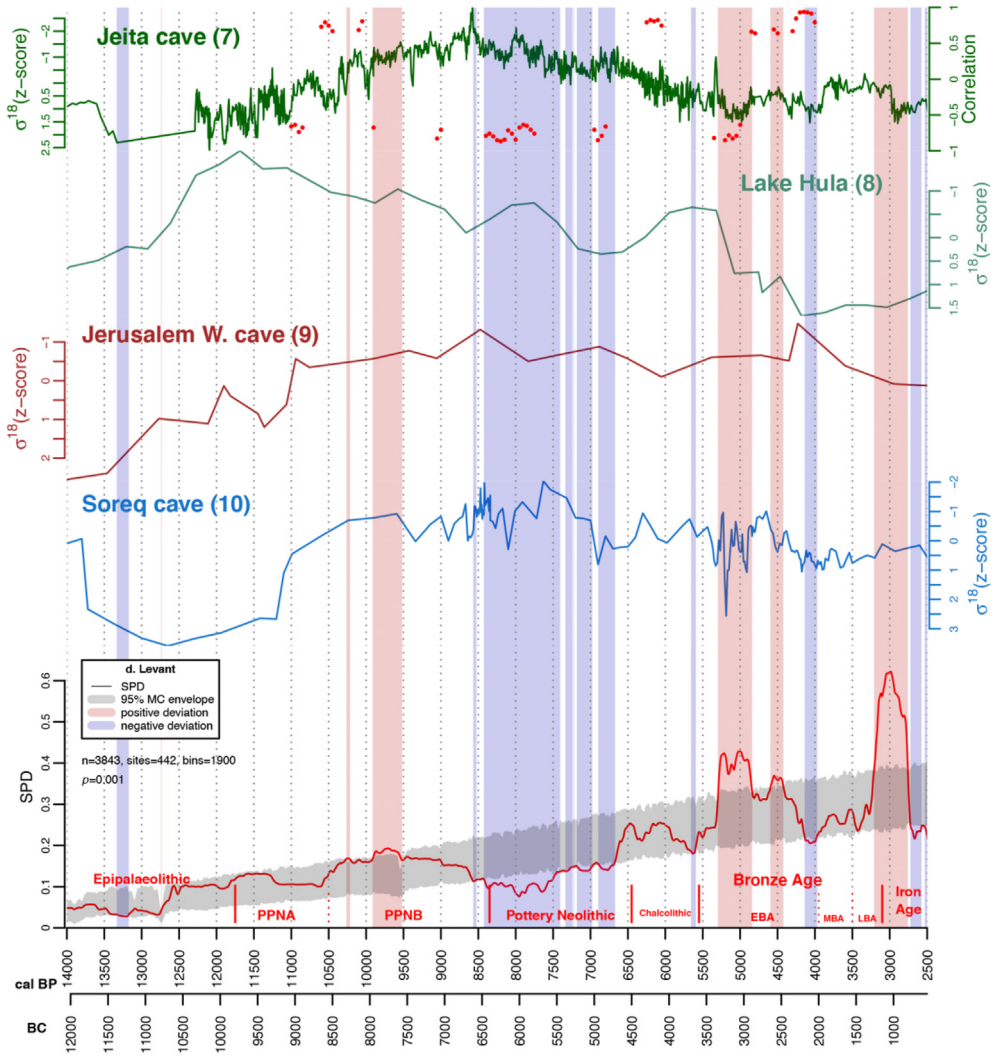

Fig. 10. SPD of unnormalised calibrated radiocarbon dates for the Levant vs. a logistic null model (95% confidence grey envelope) compared with palaeoclimate records. Blue and red vertical bands indicate respectively chronological ranges within the observed SPD deviates negatively and positively from the null model. The red dots represent significant (p-value < 0.05) positive or negative Pearson's correlations (r) values ranging from +1 to −1 by using a 500-year-time moving window. (For interpretation of the references to colour in this figure legend, the reader is referred to the Web version of this article.)

millennial scale, the regional SPDs of calibrated radiocarbon dates show population growth in concomitance with increasing wet climatic conditions during the Early Holocene (see Figs. 7, 9–12). In addition, the regional demographic trends appear to be similar during the Late Pleistocene-Early Holocene (14,000–8326 cal. yr. BP; see Table 3 and Fig. 4a) and suggest a clear relationship between population and climate among early farming communities (see Fig. 4b).

5.2. Middle Holocene (8326–4200 cal. yr. BP)

The beginning of the Middle Holocene was marked by the so-called 8.2 k cal. yr. BP event, an abrupt cold and arid episode that is visible in climate records across the whole Near East between ~8250 and 8000 cal. yr. BP (see Table 12). However, the inferred demographic trends seem to indicate that this climatic shift did not severely impact Near Eastern communities, and there is no evidence of a widespread abandonment of settlements. The population levels were quite steady in all regions with a slight decrease in Mesopotamia and Levant (Fig. 3:d-e), while Iran experienced an increase in population (Fig. 3f). The decline in the Levant began at around 8600 cal. yr. BP onwards and is unlikely to be linked to the 8.2 cal. yr. BP event. Given the prevailing stable warm and wet climatic conditions, our data supports the hypothesis that the abandonment of the Late Pre-Pottery Neolithic B (PPNB) farming villages was endogenous and related to the overexploitation of local resources after the substantial population increase at the onset of the PPNB (Goring-Morris and Belfer-Cohen 2010; Finlayson 2013, 130). Alternatively, the pronounced sub-centennial rainfall fluctuations between moist and dry conditions occurring between 9500 and 8000 cal. yr. BP (visible in the higher resolution climate records from Jeita and Soreq caves; Fig. 10:7,10) could have affected the fragile socio-economic systems of the Levantine communities (Bar-Yosef 2002; Stein et al., 2010). However, the overall drop in rainfall between 8250 and 8000 cal. yr. BP was relatively low across the whole Near East, and it is possible that Neolithic societies could have overcome this change through adaptation strategies such as the diversification of subsistence practices and storage facilities (Flohr et al., 2016, 35–36).

After the 8.2 kya event, the Middle Holocene trend was for a gradual shift towards more arid climatic conditions, with a more marked drying after ~7000 cal. yr. BP (see Fig. 6). In this context, we

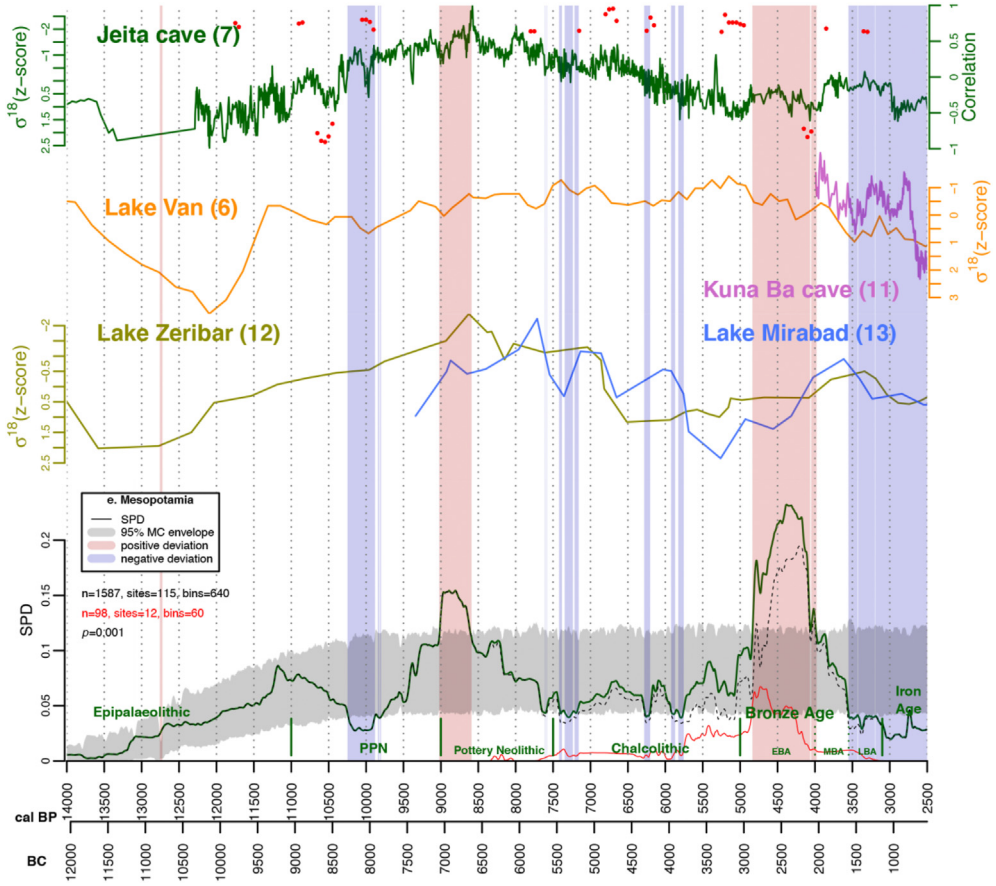

Fig. 11. SPD of unnormalised calibrated radiocarbon dates for Mesopotamia vs. a logistic null model (95% confidence grey envelope) compared with palaeoclimate records. Blue and red vertical bands indicate respectively chronological ranges within the observed SPD deviates negatively and positively from the null model. The red dots represent significant (p-value < 0.05) positive or negative Pearson's correlations (r) values ranging from +1 to −1 by using a 500-year-time moving window. (For interpretation of the references to colour in this figure legend, the reader is referred to the Web version of this article.)

have increasing regionalisation in the demographic and climatic trends. The only regions that show similar population dynamics are Anatolia and Mesopotamia (see Fig. 3: a, e; Table 3), where we see a gradual demographic decline from 8000 cal. yr. BP onwards followed by a substantial demographic boom during the Late Chalcolithic and Early Bronze Age between ~5500 and 4200 cal. yr. BP. A decline in population in these regions seems to be synchronous with a multi-millennial drying phase that was characterised by severe and rapid aridification after 7000 cal. yr. BP (see Figs. 7 and 11). This population pattern, visible not only from the SPDs of radiocarbon dates but also from the time-series of archaeological survey data (as raw count, estimated size, and probabilistic weights; see Fig. 5a–c; cf. Ur 2013; Alcock 2017; Lawrence et al., 2017), indicate that a substantial drying phase during the middle Chalcolithic could have triggered settlement abandonment and a relocation of agro-pastoral communities to areas with more stable and abundant resources, such as the Orontes river valley (Clarke 2016, 113). However, during the Late Chalcolithic and the Early Bronze Age (~5500 and 4300 cal. yr. BP.) the population grew dramatically in Anatolia and Mesopotamia despite a more arid climate (Clarke 2016, 114). In this period, the societies in Anatolia and Mesopotamia became more adaptive to climate change through technological advancements in metal manipulation, subsistence strategies and logistic infrastructure (Rosen 2007), as well as sophisticated social organisation. This period saw the emergence of large urban centres exceeding 100 ha and polities characterised by complex social hierarchies (cf. Allcock 2017; McMahon 2019). Urban-based institutions may have facilitated resilience by integrating diverse economic spheres enabling risk pooling (Wilkinson et al., 2014).

Unlike Anatolia and Mesopotamia, in the Levant population started increasing from the mid-seventh millennium cal. yr. BP when cultural changes and successful adaptations culminated in more complex societies and villages exceeding 10 ha (see Figs. 5c and 10; Levy 1998; Rowan 2013). After a decline at 5600 cal. yr. BP, the population grew dramatically during the EBA I-II (ca. 5300-4800 cal. yr. BP) despite drier climatic conditions cf. (Finkelstein 1994; Finkelstein and Gophna 1993; Palmisano et al., 2019). This may be linked to specialised agricultural production, especially olives, and more integrated regional economies (Badreshany et al., 2019). Overall population levels remained relatively high during the fifth-millennium cal. yr. BP despite a deterioration in climate, but fluctuations between 4700 and 4000 cal. yr. BP seem to be correlated strongly with the patterns drawn from the high-resolution paleoclimate records from Jeita cave (Fig. 10).

In the South Caucasus, the population boomed with the onset of the Neolithic, when the first communities of farmers settled in the Kura-Araxes interfluve cultivating domesticated cereals and practising animal husbandry (Fig. 8; Berthon 2014; Sagona 2018, 124–125). Unfortunately, we do not have paleoclimate records from the South Caucasus but it seems that a decline in population between 7000 and 5500 cal. yr. BP occurred in concomitance of a drying phase as indicated by the hydro-climate records from Karaca cave and Lake Van (Fig. 8). However, a substantial demographic

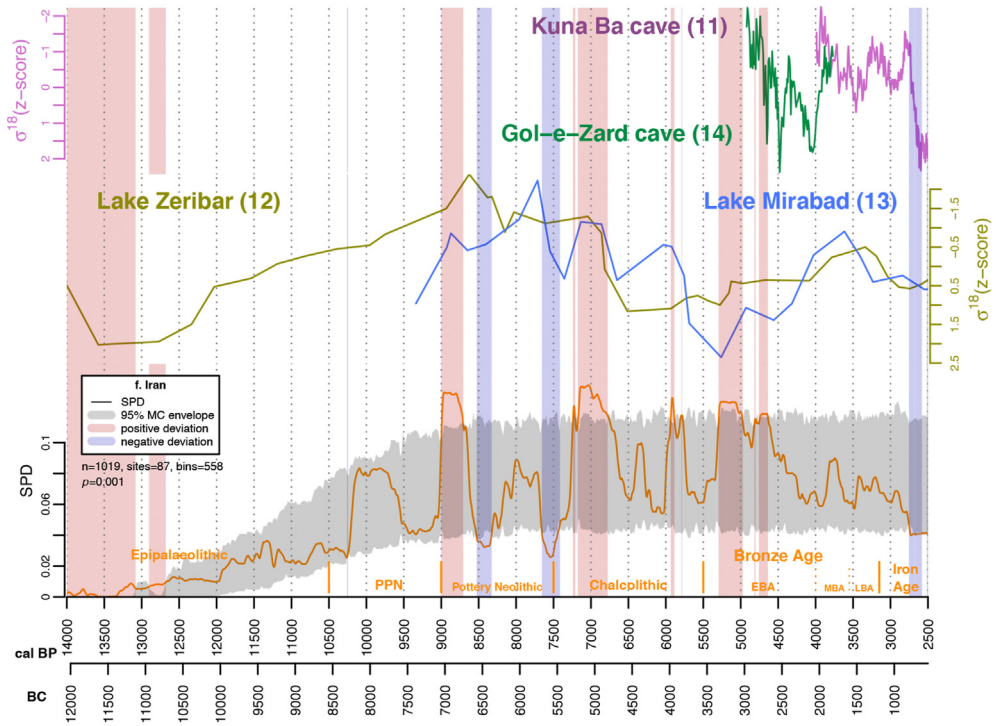

Fig. 12. SPD of unnormalised calibrated radiocarbon dates for Iran vs. a logistic null model (95% confidence grey envelope) compared with palaeoclimate records. Blue and red vertical bands indicate respectively chronological ranges within the observed SPD deviates negatively and positively from the null model. (For interpretation of the references to colour in this figure legend, the reader is referred to the Web version of this article.)

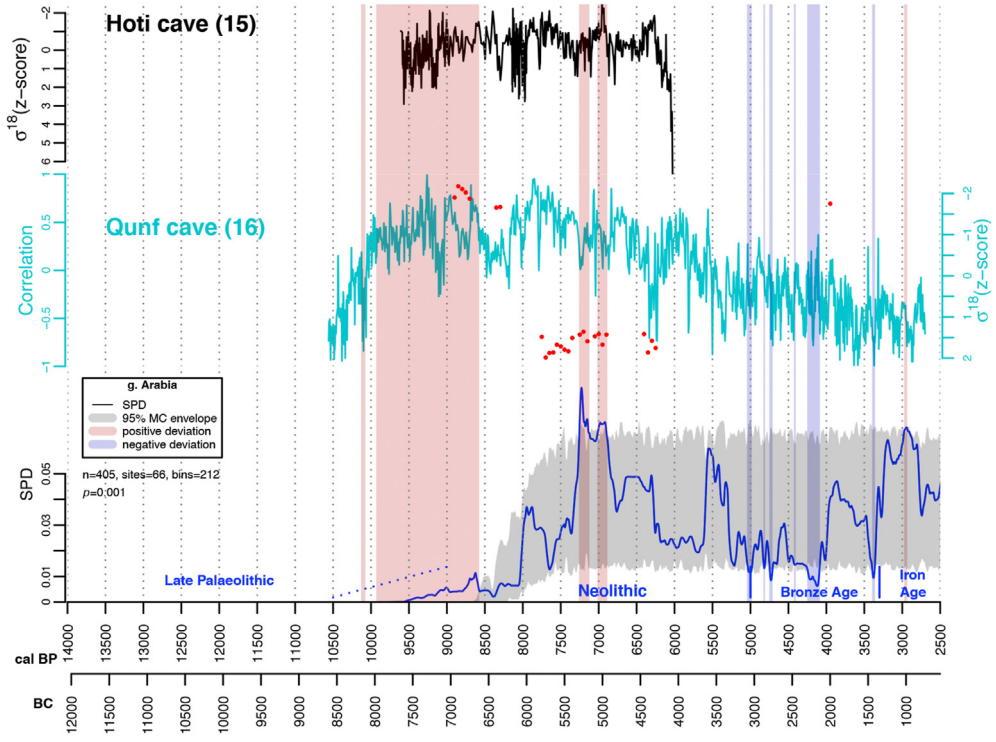

Fig. 13. SPD of unnormalised calibrated radiocarbon dates for Arabia vs. a logistic null model (95% confidence grey envelope) compared with palaeoclimate records. Blue and red vertical bands indicate respectively chronological ranges within the observed SPD deviates negatively and positively from the null model. The red dots represent significant (p-value < 0.05) positive or negative Pearson's correlations (r) values ranging from +1 to −1 by using a 500-year-time moving window. (For interpretation of the references to colour in this figure legend, the reader is referred to the Web version of this article.)

increase occured during the Bronze Age and peaked between 5000 and 4500 cal. yr. BP when the climate shifts abruptly towards more arid climatic conditions (Fig. 8).

We do not have palaeoclimate records from Cyprus and we rely on the closest available records from the Levant. The population level appears to be low at the beginning of the Middle Holocene with substantial growth in the late ceramic Neolithic between 6300 and 6000 cal. yr. BP when large villages with evidence of storage facilities and social stratification predominated (Peltenburg 1996, Fig. 9). However, a marked aridification occurred at around 6000 cal. yr. BP at the same time as a widespread abandonment of villages and a switch from agro-pastoralism to hunting, perhaps as a response to resource depletion and climatic stress (Knapp et al., 1994; Clarke 2016, 110). In the Late Chalcolithic and the EBA (5000–4000 cal. yr. BP), the population increased again as farming strategies became more intensive with greater evidence of increased livestock numbers, storage facilities and advancements in food-processing technology (Peltenburg 1998; Webb 2014).

In Iran, unlike the other regions, there was no gradual decline of the population with the shift towards more arid climatic conditions. It seems that during the Middle Holocene the population experienced booms and bust in coincidence with wet and dry climatic oscillations as shown by the palaeoclimatic records from the lakes Zeribar and Mirabad (see Fig. 12). As for the other regions, the more complex Bronze Age societies of Iran were more resilient to climatic variations and experienced a substantial demographic boom despite a rapid shift to a more arid drying phase between 5300 and 4500 cal. yr. BP (Fig. 12).

In the Arabian Peninsula, the "Holocene moist phase" between 8200 and 6200 cal. yr. BP could have favoured the rise of rich ecological niches that provided the basis for successful subsistence strategies and human settlement (Magee 2014, 42–45). In this context, an increase of population during the Neolithic could be related either to the migration of pastoralist groups looking for fertile grassland from the southern Levant to Arabia (cf. Köhler-Rollefson 1992, 13–14) or to the autochthonous development of the Neolithic package that allowed successful subsistence strategies triggering a substantial demographic growth (Cleuziou and Tosi 2007; Crassard 2009; see Fig. 13). After 6200 cal. yr. BP population dropped severely as a consequence of an abrupt drying phase that could have undermined the fragile eco-systems on which local Neolithic communities relied. Our data show an approximate correspondence with the so-called 'Dark Millennium', from 5900 to 5300 cal. yr. BP when arid conditions precluded mobile pastoral opportunities causing the abandonment of much of the peninsula (Petraglia et al., 2020). After a new demographic increase between 5600 and 5300 cal. yr. BP the population declined sharply during the Late Neolithic and the EBA at the same time as pronounced subcentennial oscillations between wet and dry episodes superimposed onto an overall more arid climate (Fig. 13).

5.3. Late Holocene (4200–2500 cal. yr. BP)

The Late Holocene was the most arid period across the chronological spectrum analysed in this study. The onset of this period was characterised by the so-called 4.2 k. cal. yr. BP event, an abrupt shift towards more arid climate conditions and dry and wet episodes between 4300 and 3800 cal. yr. BP. The magnitude, duration and impact of this event has been much debated, with significant variation in each visible across the Near East (Weiss et al., 1993; Riehl et al., 2014; Weiss 2016 and 2017; Kaniewski et al., 2018; Cookson et al., 2019; see Fig. 6). The SPDs of calibrated radiocarbon date show a substantial drop in population during the 4.2 ka cal. yr. BP event in all the Near Eastern regions (Fig. 3) with the exception of Cyprus which experienced demographic growth (see Fig. 9). The patterns visible in the SPD are less evident in the archaeological survey data, although they are present in Anatolia and Mesopotamia (Fig. 5a and c). In the Levant, the settlement data do not show a sharp decline in population but rather continuity (Fig. 5b). It may be that the comparative precision of the SPD dataset allows us to identify short term events which are not resolvable in settlement pattern data based on ceramic typologies. For example, the chronological period known as the Late Third Millennium in Mesopotamia and EBA IV in the Levant spans 4500 and 4000 cal. yr. BP (cf. Regev et al., 2012; Höflmayer et al., 2014; Ur 2010), meaning settlements occupied before, during and after an event at 4.2 k. cal. yr. BP could be conflated. The widespread decline in population should also be considered in relation to the end of the Middle Holocene, when, despite a more arid climate, Bronze Age Near Eastern communities experienced a demographic boom. An explanation could be that the rapid expansion of new large sites established in climatically marginal zones and sustained by a population drawn from outlying communities could have exerted growing pressure on local resources (cf. Wilkinson et al., 2014; Lawrence and Wilkinson 2015). As a consequence, an abrupt deterioration of the climatic conditions of even a small magnitude could have had a great impact on the stability of communities and large urban centres reliant on intensive agricultural production to feed large populations (Weiss et al., 1993; Wilkinson 1997; Wilkinson et al., 2007; Ur 2010; Massa and Şahoğlu 2015; Schwartz 2017; Altaweel and Palmisano 2019; Cookson et al., 2019). A decline in precipitation at the end of the fifth-millennium cal. yr. BP resulted in drought stress to crops and reduced yields that may have caused a shortage of food and then triggered a domino effect leading to famine, migration and societal conflict (Ur 2010: Riehl 2012; Riehl et al., 2014). However, mitigation and adaptative strategies such as the switch to more drought-tolerant crop species and from agricultural to pastoral resources avoided the total collapse of urban centres that, nevertheless, shrank in size (eg. Tell Brak, Tell Mozan; Riehl 2008; Krakauker 2010; Riehl et al., 2012; Wilkinson et al., 2014). It is worth noting that the population after the collapse was still well within the expected values for an exponential growth model, while the final part of the Middle Holocene represents a substantial positive deviation. We might then consider the boom period of urbanisation in the Early Bronze Age to be the outlier, with 'collapse' representing a return to more sustainable population levels.

After the decline in population visible across the Near East between ~4300 and 3800 cal. yr. BP (Fig. 2:c-d), the SPDs of calibrated radiocarbon dates indicate strikingly different regional patterns (Table 5; Fig. 4a). It seems that different geo-cultural areas experienced a variety of socio-ecological trajectories which are reflected in their demographic signal. However, this pattern should be considered cautiously given that in Anatolia and northern Mesopotamia we have detected no good agreement between SPDs and settlements derived proxies after 4000 cal. yr. BP (see Fig. 5:a and c). The following period saw a slight increase in precipitation between ~3800 and 3200 cal. yr. BP within an overall drying phase (Grant et al., 2012; Burstyn et al., 2019). In this context, Near Eastern communities seem to flourish again, as witnessed by an increase of the population in several regions (Fig. 3). From 4000 cal. yr. BP onwards, the SPDs tend to underestimate real population levels as archaeologists increasingly rely on ceramic dating methods. The archaeological survey data for Anatolia indicate an increase in population during the Middle Bronze Age and a peak during the Late Bronze Age with the establishment of the Hittite Empire (cf. Allcock 2017; Woodbridge et al., 2019, Fig. 5a). The Levant and Mesopotamia were characterised by patterns of demographic boom

in the MBA (~4000-3600 cal. yr. BP) and Iron Age (3200–2600 cal. yr. BP) punctuated by a decline in population in the LBA between ~3500 and 3200 cal. yr. BP (see Finkelstein 1996; Ur 2013; Lawrence et al., 2017; Palmisano et al., 2019, Fig. 5b and c and 10-11). The so-called 3.2 k cal. yr. BP event seems not to have impacted so severely on the demographic trends in the Near East between 3200 and 2900 cal. yr. BP. However, there were different regional responses. Anatolia was strongly impacted by the 3.2 k cal. yr. BP, which may have amplified the internal conflict and weakening of the Hittite Empire at the end of the LBA (Yakar 1993; Allcock 2017, 77; Kaniewski et al., 2015 and 2019; Woodbridge et al., 2019, Figs. 4a and 6). In contrast, the Levant was characterised by increases in population during the IA I-II (~3100–2700 cal. yr. BP; Figs. 4b and 9). This period was characterised by the end of the Egyptian and Hittite domination in the southern and northern Levant respectively, enabling the establishment of medium-sized regional kingdoms such as Israel, Judah, Moab, Edom, Ammon and Phoenician city-states in Lebanon (Palmisano et al., 2019). In Mesopotamia, the SPD curve likely overstates a real decline in the Late Bronze Age but fails to capture a demographic peak during the expansionist phase of the Assyrian Empire facilitated by the rapid growth of imperial capitals and a transformation of the rural landscape (Wilkinson et al., 2005; Lawrence et al., 2016; Düring 2018, Figs. 5c and 11).

Elsewhere, highly divergent trajectories also suggest political and technological changes seem to have had more of an impact than climate. In Iran, an interplay of different factors, including the end of the Shutrukid Dynasty due to the military defeat against the Babylonian king Nebuchadnezzer I and drier climatic conditions could have caused a demographic crisis and the subsequent abandonment of urban centres, political fragmentation and increasing pastoralism (Potts 1999, 370–305; Álvarez-Mon 2012, 754–755; Fig. 11). By contrast in the South Caucasus, the period between LBA and IA I (3500–2800 cal. yr. BP) was characterized by increased social complexity and the intensification of agriculture through the use of irrigation. This may be seen as a successful adaptative strategy to cope with the multimillennial drying phase of the Late Holocene (Sagona 2018, 378–379; Fig. 8) and helped to produce a demographic boom. Late Bronze Age Cyprus was characterised by significant social changes culminating in the increase of new settlements and urban centres and an apparent societal upheaval resulting in the abandonment of several Middle Cypriot settlements (Knapp 1997; Steel 2013, 865–870). Although the 3.2 k cal. yr. BP event may be implicated here (Kaniewski et al., 2019), Cyprus does not seem to have been affected by an island-wide demographic crisis since some sites such as Enkomi and Kition continued, and Aegean migrants settled along the coastal regions where polities survived and new trading harbours such as Amathus and Kourion were established (Iacovou 2008, 640; Fig. 9). In the Arabian Peninsula, we can see a negative correlation between climate and population, with the latter increasing substantially despite a drying trend (Fig. 13). In fact, the deteriorating climatic conditions during the Late Holocene could have acted as a stimulus to innovation for the Bronze Age and Iron Age communities. Major shifts in settlement and social organisation were brought by the domestication of the dromedary camel, an excellent resource of meat and dairy products, and later the adoption of the qanat or falaj, a system of subterranean irrigation channels (Boucharlat and Lombard 1985; Magee 2014, 197–222).

5.4. The decoupling of climatic and demographic trends and the impact of RCCs

The dramatic increase of population with the onset of the Holocene in the Early Neolithic is correlated positively with a trend towards wetter climatic conditions that could have favoured the diachronous demic diffusion of farming from the Levant (~11,700 cal. yr. BP) to the South Caucasus by 8000 cal. yr. BP. Unlike the Early Holocene, characterised by a growing population, in the Middle Holocene we see cycles of demographic booms and busts, some of which are synchronous with short periods of amelioration or deterioration of climatic conditions (Clarke et al., 2016). During the second half of the Middle Holocene (~5500 cal. yr. BP), and into the Later Holocene, we can identify a decoupling of climate and human population. The climatic and demographic trends, despite regional variations, are either negatively correlated or not correlated at all (Fig. 4b). We interpret this as due to technological advancement and the building up of infrastructure of more complex societies less vulnerable to a more arid climate (Lawrence et al., 2016; Roberts et al., 2019).

During the Early and Late Holocene RCC events seems to have exerted a minor impact on Near Eastern Communities. While the 10.2 k cal. yr. BP event seems to have determined a cultural break in the local communities in Upper Mesopotamia and northern Levant (Borrell et al., 2015), the 9.2 k and 8.2 k cal. yr. BP events do not appear to be linked to a decline population or a broad abandonment of settlements (Flohr et al., 2016). On the other hand, despite the decoupling between population and climate during the second half of the Middle Holocene, the 4.2 k cal. yr. BP event seems to have exerted a dramatic impact on Near Eastern communities and caused a widespread demographic crisis. In this instance the abandonment of settlements or their reduction in size is perhaps the result of the interplay between unfavourable climatic conditions and a system of large urban centres that grew rapidly during the Early Bronze Age and were reliant on fragile systems of food provision (Wilkinson et al., 2014; Lawrence and Wilkinson 2015). The collapse in population visible during this RCC event should therefore be viewed in the context of the preceding demographic boom. The impact of the 3.2 ka cal. yr. BP event was more regionalised and did not affect population patterns across the whole Near East in the same way as the 4.2 cal. yr. BP event. The Late Bronze Age collapse may have impacted specific polities, such as the Hittite and Egyptian empires, but social and technological capacity was retained, and new political entities, such as the emergent kingdoms of the Levant, were able to sustain high populations (Rosen 2007, 101–102). We might speculate that as societies become increasingly affluent and complex, straightforward demographic proxies are less useful in demarcating responses to RCC events. Such societies may be capable of maintaining food production at a level which prevents large scale site abandonment or mortality, and therefore visibility in the sorts of proxies we have used in this paper, while still experiencing dramatic shifts in material wealth and social and political organisation.

6. Conclusions

This paper has highlighted, for the first time, the correlations between demographic and climatic trends from the Late Pleistocene to the Late Holocene (14,000–2500 cal. yr. BP) across the Near East. To do so, we used most of the known and freely accessible palaeoclimatic records available for the area and three types of archaeo-demographic proxies (radiocarbon dates, settlement estimated size, raw site counts). We argue that population trends are best estimated using a multi-proxy approach in order to compare independent archaeological indices and statistically assess to what extent they correlate with one another. This approach allows us to explore the strengths and weaknesses of each line of evidence and to build more robust narratives, both in the very long run and in specific well-defined periods. Unfortunately, high quality

integrated datasets of archaeological settlement data are not (yet) available across the whole Near East. However, the overall agreement between the SPDs of calibrated radiocarbon dates and the settlement-based proxies for three sub-regions (South-central Anatolia, Southern Levant, and Upper Mesopotamia) suggests SPDs can be a good indicator for reconstructing past population dynamics during particular periods. SPDs can be used up to ~2800 cal. yr. BP as a good indicator, while archaeological survey data can extend until more recent periods (e.g. Medieval). In some regions, such as Anatolia, Mesopotamia and Iran, SPDs tend to underestimate the population from around ~4000-3500 cal. yr. BP when compared with the settlement derived proxies. However, archaeological settlement derived proxies have the opposite problem of "dwarfing" population levels in the earlier periods, especially before the widespread use of pottery. Where they can be confidently interpreted, the chronological precision available through SPDs of radiocarbon dates mean they are a useful addition to settlement data for comparison with palaeoclimatic records, especially in relation to very short term 'events'. Given the patchiness of the available data, we are aware of the caveats in inferring population trends by using only SPDs of calibrated radiocarbon dates and our results should be considered as a preliminary assessment.

The long-term demographic trends show similar trajectories between regions in the Late Pleistocene-Early Holocene (14,000–8326 cal. yr. BP), increasing regionalisation of demographic patterns in the Middle Holocene (8326–4200 cal. yr. BP), and marked inter-regional contrasts during the Late Holocene (4200–2500 cal. yr. BP). Comparisons between palaeoclimatic and demographic proxies have revealed either no statistical correlation or an overall negative correlation between population fluctuations and hydro-climate patterns when taking into account the whole chronological scope between 14,000 and 2500 cal. yr. BP. In other words, human populations grew and declined independently from long-term climate trajectories, and possible correlations are only visible for shorter periods. Unfortunately, most of the available hydro-climate patterns available for the Near East have a mean sampling interval greater than 150 years and, therefore, only a few of them make it possible to assess the correlations between climate and population for short periods. In addition, the patchiness of the available hydro-climate records and their dispersed spatial distribution means coherent spatial and chronological comparisons with the archaeo-demographic proxies are not always possible.

Although we have highlighted general trends suggesting a good correlation between climate and population during the Early Holocene and a decoupling from the second half of the Middle Holocene, the Near East shows a wide spectrum of regional socio-ecological trajectories. For instance, the transition from the Late Pleistocene to the early Holocene was characterised by high regional variation, with the Levant and Mesopotamia potentially acting as refugia during the Younger Dryas stadial (~12,700–11,700 cal. yr. BP; Roberts et al., 2018), attracting population while other areas declined. This regionality is also visible in the RCCs occurring in the Early and Middle Holocene (10.2, 9.2 and 8.2 k cal. yr. BP events), all of which had a limited and differential impact across the Near East. Even the more widespread 4.2 k and 3.2 k cal. yr. BP events prompted different local responses. The 4.2 k cal. event appears to have had the greatest impact, but our results show that this must be taken in the context of a booming pre-event population which likely put pressure on resources and constrained the ability of communities to adapt. The 3.2 k. cal. event had perhaps the most regionalised impact of all. This might reflect the generally increasing robustness of food production systems in the face of climate fluctuations on the one hand, and the growing importance of social and especially political organisation as factors in resilience levels on the other.

Future research efforts will focus on the integration of the SPDs of calibrated radiocarbon dates with multiple archaeo-demographic proxies (raw site count, aggregated estimated settlement size, number of burials) covering the whole Near East in order to deliver more robust results and reconstruct population dynamics over a chronological spectrum extending up to Medieval and post-Medieval times. Additional archaeological datasets would also enable a more detailed investigation of the individual regional trends identified here.

It is clear from the present work that while a wealth of archaeological data exist across the Near East, a higher number of well dated palaeoclimatic archives are needed to provide a more even spatial and chronological coverage, and to produce more accurate interpretations of past human-climate interactions. The subdivision of our seven geo-cultural regions is justified on the basis of traditional research trajectories, real differences in physical geography and by the need to guarantee sufficient data to produce meaningful results. However, an increase in the spatial resolution of available palaeoclimatic data would allow us to subdivide further, and potentially to assess relationships across a wider range of environments. This would allow to assess how social behaviours changed in different ecological niches. Furthermore, the integration of vegetation pollen-based reconstruction would allow us to assess not only correlations between climate and population but also the impact of climate and population change on vegetation and the wider landscape.

Author statement

Alessio Palmisano: Conceptualization, Methodology, Software, Formal analysis, Investigation, Data curation, Writing – original draft, Writing – review & editing, Visualization. Dan Lawrence: Conceptualization, Writing – original draft, Writing – review & editing, Supervision, Project administration, Funding acquisition. Michelle W. de Gruchy: Data curation, Writing – review & editing. Andrew Bevan: Methodology, Data curation, Writing – review & editing. Stephen Shennan: Data curation, Writing – review & editing.

Declaration of competing interest

The authors declare that they have no known competing financial interests or personal relationships that could have appeared to influence the work reported in this paper.

Acknowledgements

This research was supported by the European Research Council under the European Union's Horizon 2020 research and innovation programme for the project "CLaSS – Climate, Landscape, Settlement and Society: Exploring Human Environment Interaction in the Ancient Near East" (grant number 802424, award holder: Dan Lawrence).

We are grateful to Steven Savage and Thomas Levy for allowing us to use a large portion of data from The Digital Archaeological Atlas of the Holy Land (DAAHL; https://daahl.ucsd.edu/DAAHL/).

Appendix A. Supplementary data and codes

The dataset included here provides a collection of archaeo-demographic (radiocarbon dates and archaeological settlement data) and palaeoclimatic proxies from the Late Pleistocene to the Late Holocene. In addition, the digital archive related to this paper allows reproducible analyses and figures in the form of four scripts written in R statistical computing language. The digital archive is

freely available at the following link via the repository Zenodo: http://doi.org/10.5281/zenodo.4322979.

Appendix B. Supplementary data

Supplementary data to this article can be found online at https://doi.org/10.1016/j.quascirev.2020.106739.

References

Adams, R.M., 1965. Land behind Baghdad: A History of Settlement on the Diyala Plains. Chicago University Press, Chicago.

Adams, R.M., 1981. Heartland of Cities. Surveys of Ancient Settlement and Land Use on the Central Floodplain of the Euphrates. University of Chicago Press, Chicago.

Allcock, S.L., 2017. Long-term socio-environmental dynamics and adaptive cycles in Cappadocia, Turkey during the Holocene. Quat. Int. 446, 66–82.

Altaweel, M., Palmisano, A., 2019. Urban and transport scaling: northern Mesopotamia in the late chalcolithic and Bronze age. J. Archaeol. Method Theor 26, 943–966.

Álvarez-Mon, J., 2012. Elam: Iran's first empire. In: Potts, D.T. (Ed.), A Companion to the Archaeology of the Ancient Near East. Wiley-Blackwell, London, pp. 740–757.

ArAGATS project, 2019. ArAGATS Data Portal. Available at: https://aragats.gorgesapps.us//. (Accessed 10 November 2019).

Asouti, E., Fuller, D.Q., 2012. From foraging to farming in the southern Levant: the development of Epipalaeolithic and Pre-Pottery Neolithic plant management strategies. Veg. Hist. Archaeobotany 21 (2), 149–162.

Atsawawaranunt, K., Harrison, S., Comas-Bru, L., 2019. SISAL (Speleothem Isotopes Synthesis and AnaLysis Working Group) Database Version 1b. Dataset. https://doi.org/10.17864/1947.189.

Bader, N.O., 1993. Tell maghzaliyah, an early neolithic site in northern Iraq. In: Yoffee, N., Clark, J.J. (Eds.), Early Stages in the Evolution of Mesopotamian Civilization: Soviet Excavations in the Sinjar Plain, Northern Iraq. University of Arizona Press, Tucson, pp. 7–40.

Badreshany, K., Philip, G., Kennedy, M., 2019. The development of integrated regional economies in the Early Bronze Age Levant: new evidence from Combed-Ware jars. Levant 51, 1–37.

Baird, D., Fairbairn, A., Martin, L., Middleton, C., 2012. the Boncuklu Project; the origins of sedentism, cultivation and herding in central Anatolia. In: Ozdogan, M., Bas, gelen.N. (Eds.), *The Neolithic in Turkey: New Excavations and New Research*. Istanbul: Arkeoloji Ve Sanat Taslikliоglu, pp. 219–244.

Baker, A., Hartmann, A., Duan, W., et al., 2019. Global analysis reveals climatic controls on the oxygen isotope composition of cave drip water. Nat. Commun. 10, 2984.

Bar-Matthews, M., Ayalon, A., Gilmour, M., Matthews, A., Hawkesworth, C.J., 2003. Sea–land oxygen isotopic relationships from planktonic foraminifera and speleothems in the Eastern Mediterranean region and their implication for paleorainfall during interglacial intervals. Geochem. Cosmochim. Acta 67 (17), 3181–3199.

Bar-Yosef, O., 2002. The Natufian culture and the early Neolithic: social and economic trends in southwestern Asia. In: Belwood, P., Renfrew, C. (Eds.), Examining the Farming/Language Dispersal Hypothesis. University of Cambridge, Cambridge, pp. 113–126.

Becerra-Valdivia, L., Leal-Cervantes, R., Wood, R., Higham, T., 2020. Challenges in sample processing within radiocarbon dating and their impact in 14C-dates-as-data studies. J. Archaeol. Sci. 113, 105043.

Belfer-Cohen, A., Bar-Yosef, O., 2000. Early sedentism in the Near East: a bumpy ride to village life. In: Kujit, I. (Ed.), *Life in Neolithic Farming Communities: Social Organization, Identity and Differentiation*. Kluwer Academic/Plenum Publishers, New York, pp. 19–37.

Bellwood, P., 2013. First Migrants: Ancient Migration in Global Perspective. Wiley-Blackwell, London.

Benz, M., 2014. PPND – the platform for neolithic radiocarbon dates. Available at: https://www.exoriente.org/associated_projects/ppnd.php.

Berger, J.F., Shennan, S., Woodbridge, J., Palmisano, A., Mazier, F., Nuninger, L., Guillon, S., Doyen, E., Bégeot, C., Andrieu-Ponel, V., Azuara, J., 2019. Holocene land cover and population dynamics in Southern France. Holocene 29 (5), 776–798.

Berthon, R., 2014. Past, current, and future contribution of zooarchaeology to the knowledge of the Neolithic and Chalcolithic cultures in South Caucasus. Studies in Caucasian Archaeology 2, 4–30.

Bettencourt, L.M.A., Lobo, J., Helbing, D., Kuhnert, C., West, G.B., 2007. Growth, innovation, scaling, and the pace of life in cities. Proc. Natl. Acad. Sci. Unit. States Am. 104 (17), 7301–7306.

Bevan, A., Crema, E.R., 2020. Rcarbon v1.4.1: Calibration and Analysis of Radiocarbon Dates. /. https://CRAN.R-project.org/package=rcarbon.

Bevan, A., Colledge, S., Fuller, D., Fyfe, R., Shennan, S., Stevens, C., 2017. Holocene fluctuations in human population demonstrate repeated links to food production and climate. Proc. Natl. Acad. Sci. Unit. States Am. 114 (49), E10524–E10531.

Bevan, A., Palmisano, A., Woodbridge, J., Fyfe, R., Roberts, C.N., Shennan, S., 2019. The changing face of the Mediterranean–Land cover, demography and environmental change: introduction and overview. Holocene 29 (5), 703–707.

Binford, L.R., 1968. Post-Pleistocene adaptations. In: Binford, S.R., Binford, L.R. (Eds.), New Perspectives in Archaeology. Aldine Publishing Company, Chicago, pp. 313–341.

Bini, M., Zanchetta, G., Persoiu, A., Cartier, R., Català, A., Cacho, I., Dean, J.R., Di Rita, F., Drysdale, R.N., Finnè, M., Isola, I., Jalali, B., Lirer, F., Magri, D., Masi, A., Marks, L., Mercuri, A.M., Peyron, O., Sadori, L., Sicre, M.A., Welc, F., Zielhofer, C., Brisset, E., 2019. The 4.2 ka BP event in the mediterranean region: an overview. Clim. Past 15 (2), 555–577.

Böhner, U., Schyle, D., 2006. Radiocarbon CONTEXT Database 2002-2006. Available at: http://context-database.uni-koeln.de.

Borrell, F., Junno, A., Barceló, J.A., 2015. Synchronous environmental and cultural change in the emergence of agricultural economies 10,000 years ago in the Levant. PloS One 10 (8), e0134810.

Boserup, E., 1965. The Condition of Agricultural Growth. The Economics of Agrarian Change under Population Pressure. Allan and Urwin, London.

Boucharlat, R., Lombard, P., 1985. The oasis of al-ain in the Iron age – excavations at rumeilah, 1981–1983: survey at hili 14. Archaeology in the United Arab Emirates 4, 44–73.

Brami, M.N., 2015. A graphical simulation of the 2,000-year lag in Neolithic occupation between Central Anatolia and the Aegean basin. Archaeological and Anthropological Sciences 7 (3), 319–327.

Burstyn, Y., Martrat, B., Lopez, J.F., Iriarte, E., Jacobson, M.J., Lone, M.A., Deininger, M., 2019. Speleothems from the Middle East: an example of water limited environments in the SISAL database. Quaternary 2 (2), 16.

Campbell, S., 2012. Northern Mesopotamia. In: Potts, D.T. (Ed.), A Companion to the Archaeology of the Ancient Near East. Wiley-Blackwell, London, pp. 415–430.

Cappers, R.T.J., Bottema, S., Bar-Yosef, O., Belfer-Cohen, A., 2002. Facing environmental crisis. Societal and cultural changes at the transition from the Younger Dryas to the Holocene in the Levant. In: Cappers, R.T.J., Bottema, S. (Eds.), The Dawn of Farming in the Near East, Studies in Early Near Eastern Production, Subsistence, and Environment, vol. 6. Ex Oriente, Berlin, pp. 55–66.

Carneiro, R.L., 1962. Scale analysis as an instrument for the study of cultural evolution. SW. J. Anthropol. 18 (2), 149–169.

Carolin, S.A., Walker, R.T., Day, C.C., Ersek, V., Sloan, R.A., Dee, M.W., Talebian, M., Henderson, G.M., 2019. Precise timing of abrupt increase in dust activity in the Middle East coincident with 4.2 ka social change. Proc. Natl. Acad. Sci. Unit. States Am. 116 (1), 67–72.

Casana, J., 2009. Alalakh and the archaeological landscape of Mukish: the political geography and population of a Late Bronze Age kingdom. Bull. Am. Sch. Orient. Res. 353 (1), 7–37.

CDRC, 2016. Banadora (BAnque NAtionale de DOnnées RAdiocarbone pour l'Europe et le Proche Orient). Centre de Datation par le Radiocarbone de Lyon (CDRC). Available at: http://www.arar.mom.fr/banadora/. (Accessed 31 May 2018).

Cheng, H., Fleitmann, D., Edwards, R.L., Wang, X., Cruz, F.W., Auler, A.S., Mangini, A., Wang, Y., Kong, X., Burns, S.J., Matter, A., 2009. Timing and structure of the 8.2 kyr BP event inferred from δ18O records of stalagmites from China, Oman, and Brazil. Geology 37 (11), 1007–1010.

Cheng, H., Sinha, A., Verheyden, S., Nader, F.H., Li, X.L., Zhang, P.Z., Yin, J.J., Yi, L., Peng, Y.B., Rao, Z.G., Ning, Y.F., 2015. The climate variability in northern Levant over the past 20,000 years. Geophys. Res. Lett. 42 (20), 8641–8650.

Cherry, J.F., 1983. Frogs round the pond: perspectives on current archaeological survey projects in the mediterranean region. In: Keller, D.R., Rupp, D.W. (Eds.), Archaeological Survey in the Mediterranean Region. British Archaeological Reports, Oxford, pp. 375–416.

Clarke, J., Brooks, N., Banning, E.B., Bar-Matthews, M., Campbell, S., Clare, L., Cremaschi, M., di Lernia, S., Drake, N., Gallinaro, M., Manning, S., 2016. Climatic changes and social transformations in the Near East and North Africa during the 'long' 4th millennium BC: a comparative study of environmental and archaeological evidence. Quat. Sci. Rev. 136, 96–121.

Cleuziou, S., Tosi, M., 2007. In the Shadow of the Ancestors. *The Prehistoric Foundations of the Early Arabian Civilization in Oman*. Muscat: Ministry of Heritage and Culture, Sultanate of Oman.

Cline, E.H., 2015. 1177 BC: the Year Civilization Collapsed. Princeton University Press, Princeton.

Contreras, D.A., Meadows, J., 2014. Summed radiocarbon calibrations as a population proxy: a critical evaluation using a realistic simulation approach. J. Archaeol. Sci. 52, 591–608.

Cookson, E., Hill, D.J., Lawrence, D., 2019. Impacts of long-term climate change during the collapse of the Akkadian Empire. J. Archaeol. Sci. 106, 1–9.

Crassard, R., 2009. Modalities and characteristics of human occupations in Yemen during the Early/Mid-Holocene. Compt. Rendus Geosci. 341 (8–9), 713–725.

Crema, E.R., 2012. Modelling temporal uncertainty in archaeological analysis. J. Archaeol. Method Theor 19 (3), 440–461.

Crema, E., Bevan, A., 2020. Inference from large sets of radiocarbon dates: software and methods. Radiocarbon 1–17. https://doi.org/10.1017/RDC.2020.95.

Crema, E.R., Bevan, A., Lake, M., 2010. A probabilistic framework for assessing spatio-temporal point patterns in the archaeological record. J. Archaeol. Sci. 37, 1118–1130.

Crema, E.R., Habu, J., Kobayashi, K., Madella, M., 2016. Summed probability distribution of 14 C dates suggests regional divergences in the population dynamics of the jomon period in eastern Japan. PloS One 11 (4), e0154809.

de Pablo, J.F.L., Gutiérrez-Roig, M., Gómez-Puche, M., McLaughlin, R., Silva, F., Lozano, S., 2019. Palaeodemographic modelling supports a population bottleneck during the Pleistocene-Holocene transition in Iberia. Nat. Commun. 10 (1), 1–13.

Dean, J.R., Jones, M.D., Leng, M.J., Noble, S.R., Metcalfe, S.E., Sloane, H.J., Sahy, D., Eastwood, W.J., Roberts, C.N., 2015. Eastern Mediterranean hydroclimate over the late glacial and Holocene, reconstructed from the sediments of Nar lake, central Turkey, using stable isotopes and carbonate mineralogy. Quat. Sci. Rev. 124, 162–174.
Deininger, M., McDermott, F., Mudelsee, M., Werner, M., Frank, N., Mangini, A., 2017. Coherency of late Holocene European speleothem δ18O records linked to North Atlantic Ocean circulation. Clim. Dynam. 49 (1–2), 595–618.
Demjan, P., Dreslerová, D., 2016. Modelling distribution of archaeological settlement evidence based on heterogeneous spatial and temporal data. J. Archaeol. Sci. 69, 100–109.
Drennan, R.D., Berrey, C.A., Peterson, C.E., 2015. Regional Settlement Demography in Archaeology. Eliot Werner Publications, New York.
Düring, B.S., 2018. Engineering empire: a provincial perspective on the middle assyrian empire. In: Düring, B.S., Stek, T.D. (Eds.), The Archaeology of Imperial Landscapes. A Comparative Study of Empires in the Ancient Near East and Mediterranean World. Cambridge University Press, Cambridge, pp. 21–47.
Eastwood, W.J., Leng, M.J., Roberts, N., Davis, B., 2007. Holocene climate change in the eastern Mediterranean region: a comparison of stable isotope and pollen data from Lake Gölhisar, southwest Turkey. J. Quat. Sci.: Published for the Quaternary Research Association 22 (4), 327–341.
Enzel, Y., Kushnir, Y., Quade, J., 2015. The middle Holocene climatic records from Arabia: reassessing lacustrine environments, shift of ITCZ in Arabian Sea, and impacts of the southwest Indian and African monsoons. Global Planet. Change 129, 69–91.
Feinman, G.M., 2011. Size, complexity, and organizational variation: a comparative approach. Cross Cult. Res. 45 (1), 37–58.
Finkelstein, I., 1994. The emergence of Israel: a phase in the cyclic history of canaan in the third and second millennia BCE. In: Finkelsten, I., Na'aman, N. (Eds.), From Nomadism to Monarchy: Archaeological and Historical Aspects of Early Israel. Israel Exploration Society, Jerusalem, pp. 150–178.
Finkelstein, I., 1996. Ethnicity and origin of the Iron I settlers in the highlands of Canaan: can the real Israel stand up? Biblic. Archaeol. 59 (4), 198–212.
Finkelstein, I., Gophna, R., 1993. Settlement, demographic, and economic patterns in the highlands of Palestine in the Chalcolithic and Early Bronze periods and the beginning of urbanism. Bull. Am. Sch. Orient. Res. 289, 1–22.
Finlayson, B., 2013. Introduction to the levant during the neolithic period. In: Steiner, M.L., Killebrew, A.E. (Eds.), The Oxford Handbook of the Archaeology of the Levant: C. 8000–332 BCE. Oxford University Press, Oxford, pp. 124–133.
Finné, M., Holmgren, K., Shen, C.C., Hu, H.M., Boyd, M., Stocker, S., 2017. Late Bronze age climate change and the destruction of the mycenaean palace of nestor at pylos. PloS One 12 (12), e0189447.
Finné, M., Woodbridge, J., Labuhn, I., Roberts, C.N., 2019. Holocene hydro-climatic variability in the Mediterranean: a synthetic multi-proxy reconstruction. Holocene 29 (5), 847–886.
Fisher, W.B., 2013. The Middle East (Routledge Revivals): A Physical, Social and Regional Geography. Routledge, London.
Fleitmann, D., Burns, S.J., Mangini, A., Mudelsee, M., Kramers, J., Villa, I., Neff, U., Al-Subbary, A.A., Buettner, A., Hippler, D., Matter, A., 2007. Holocene ITCZ and Indian monsoon dynamics recorded in stalagmites from Oman and Yemen (Socotra). Quat. Sci. Rev. 26 (1–2), 170–188.
Fleitmann, D., Cheng, H., Badertscher, S., Edwards, R.L., Mudelsee, M., Göktürk, O.M., Fankhauser, A., Pickering, R., Raible, C.C., Matter, A., Kramers, J., 2009. Timing and climatic impact of Greenland interstadials recorded in stalagmites from northern Turkey. Geophys. Res. Lett. 36 (19), L19707.
Flohr, P., Fleitmann, D., Matthews, R., Matthews, W., Black, S., 2016. Evidence of resilience to past climate change in Southwest Asia: early farming communities and the 9.2 and 8.2 ka events. Quat. Sci. Rev. 136, 23–39.
French, J.C., 2015. The demography of the Upper Palaeolithic hunter–gatherers of Southwestern France: a multi-proxy approach using archaeological data. J. Anthropol. Archaeol. 39, 193–209.
French, J.C., Collins, C., 2015. Upper Palaeolithic population histories of South-western France: a comparison of the demographic signatures of 14 C date distributions and archaeological site counts. J. Archaeol. Sci. 55, 122–134.
Frumkin, A., Ford, D.C., Schwarcz, H.P., 1999. Continental oxygen isotopic record of the last 170,000 years in Jerusalem. Quat. Res. 51 (3), 317–327.
Fuller, D.Q., Willcox, G., Allaby, R.G., 2012. Early agricultural pathways: moving outside the 'core area'hypothesis in Southwest Asia. J. Exp. Bot. 63 (2), 617–633.
Göktürk, O.M., Fleitmann, D., Badertscher, S., Cheng, H., Edwards, R.L., Leuenberger, M., Fankhauser, A., Tüysüz, O., Kramers, J., 2011. Climate on the southern Black Sea coast during the holocene: implications from the sofular cave record. Quat. Sci. Rev. 30 (19–20), 2433–2445.
Goldstone, J.A., 1993. Predicting revolutions: why we could (and should) have foreseen the revolutions of 1989–1991 in the USSR and eastern Europe. Content 2, 127–152.
Gophna, R., Portugali, J., 1988. Settlement and demographic processes in Israel's coastal plain from the Chalcolithic to the Middle Bronze Age. Bull. Am. Sch. Orient. Res. 269, 11–28.
Goring-Morris, A.N., Belfer-Cohen, A., 2010. Great expectations, or, the inevitable collapse of the early neolithic in the Near East. In: Bandy, M.S., Fox, J.R. (Eds.), Becoming Villagers: Comparing Early Village Societies. University of Arizona Press, Tucson, AZ, pp. 62–77.
Grant, K.M., Rohling, E.J., Bar-Matthews, M., Ayalon, A., Medina-Elizalde, M., Ramsey, C.B., Satow, C., Roberts, A.P., 2012. Rapid coupling between ice volume and polar temperature over the past 150,000 years. Nature 491 (7426), 744–747.
Greenberg, R., 2017. No collapse: transmutations of early Bronze age urbanism in the southern levant. In: Höflmayer, F. (Ed.), The Late Third Millennium in the Ancient Near East: Chronology, C14 and Climate Change; Papers from the Oriental Institute Seminar Held at the Oriental Institute of the University of Chicago, 7–8 March 2014. Oriental Institute of the University of Chicago, Chicago, IL, pp. 33–60.
Greenberg, R., Keinan, A., 2009. Israeli Archaeological Activity in the West Bank 1967-2007: A Sourcebook. Ostracon, Jerusalem.
Grootes, P.M., Stuiver, M., 1997. Oxygen 18/16 variability in Greenland snow and ice with 10– 3-to 105-year time resolution. J. Geophys. Res.: Oceans 102 (C12), 26455–26470.
Guerrero, E., Naji, S., Bocquet-Appel, J.-P., 2008. The signal of the Neolithic demographic transition in the Levant. In: Bocquet-Appel, J.-P., Bar-Yosef, O. (Eds.), *The Neolithic Demographic Transition and its Consequences*. Springer Science & Business Media, pp. 57–80.
Helwing, B., 2012. The Iranian plateau. In: Potts, D.T. (Ed.), A Companion to the Archaeology of the Ancient Near East. Wiley-Blackwell, London, pp. 501–511.
Hemming, D., Buontempo, C., Burke, E., Collins, M., Kaye, N., 2010. How uncertain are climate model projections of water availability indicators across the Middle East? Phil. Trans. Math. Phys. Eng. Sci. 368 (1931), 5117–5135.
Hinz, M., Furholt, M., Müller, J., Raetzel-Fabian, D., Rinne, C., Sjögren, K.G., Wotzka, H.P., 2012. RADON - radiocarbon dates online 2012. Central European database of ^{14}C dates for the neolithic and early Bronze age. Journal of Neolithic Archaeology 14, 1–4. Available at: http://radon.ufg.uni-kiel.de/.
Höflmayer, F., Dee, M.W., Genz, H., Riehl, S., 2014. Radiocarbon evidence for the early Bronze age levant: the site of Tell fadous-Kfarabida (Lebanon) and the end of the early Bronze III period. Radiocarbon 56 (2), 529–542.
Hole, F., 1987. Settlement and society in the village period. In: Hole, F. (Ed.), The Archaeology of Western Iran: Settlement and Society from Prehistory to the Islamic Conquest. Smithsonian Institute Press, Washington, DC, pp. 79–106.
Iacovou, M., 2008. Cultural and political configurations in Iron Age Cyprus: the sequel to a protohistoric episode. Am. J. Archaeol. 625–657.
Izdebski, A., Holmgren, K., Weiberg, E., Stocker, S.R., Buentgen, U., Florenzano, A., Gogou, A., Leroy, S.A., Luterbacher, J., Martrat, B., Masi, A., 2016. Realising consilience: how better communication between archaeologists, historians and natural scientists can transform the study of past climate change in the Mediterranean. Quat. Sci. Rev. 136, 5–22.
Johnson, A.W., Earle, T.K., 2000. The Evolution of Human Societies: from Foraging Group to Agrarian State. Stanford University Press.
Jones, M.D., Abu-Jaber, N., AlShdaifat, A., Baird, D., Cook, B.I., Cuthbert, M.O., Dean, J.R., Djamali, M., Eastwood, W., Fleitmann, D., Haywood, A., 2019. 20,000 years of societal vulnerability and adaptation to climate change in southwest Asia. Wiley Interdisciplinary Reviews: Water 6 (2), e1330.
Kaniewski, D., Van Campo, E., 2017. The 3.2 kyr BP event and the Late Bronze Age crisis, a climate-induced spiral of decline. In: Weiss, H. (Ed.), Megadrought and Collapse. Oxford University Press, Oxford, pp. 161–182.
Kaniewski, D., Guiot, J., Van Campo, E., 2015. Drought and societal collapse 3200 years ago in the Eastern Mediterranean: a review. Wiley Interdisciplinary Reviews: Climate Change 6 (4), 369–382.
Kaniewski, D., Marriner, N., Cheddadi, R., Guiot, J., Van Campo, E., 2018. The 4.2 ka BP event in the Levant. Clim. Past 14, 1529–1542.
Kaniewski, D., Marriner, N., Bretschneider, J., Jans, G., Morhange, C., Cheddadi, R., Otto, T., Luce, F., Van Campo, E., 2019. 300-year drought frames late Bronze age to early Iron age transition in the Near East: new palaeoecological data from Cyprus and Syria. Reg. Environ. Change 19 (8), 2287–2297.
Knapp, A.B., 1997. The Archaeology of Late Bronze Age Cypriot Society: the Study of Settlement, Survey and Landscape. University of Glasgow, Department of Archaeology, Glasgow.
Knapp, A.B., Held, S.O., Manning, S.W., 1994. The prehistory of Cyprus: problems and prospects. J. World PreHistory 8 (4), 377–453.
Kohler, T.A., Cole, S., Ciupe, S., 2009. Population and warfare: a test of the Turchin model in Puebloan societies. In: Shennan (Ed.), Pattern and Process in Cultural Evolution. University of California Press, Berkeley, pp. 277–295.
Krakauer, N., Cook, B.I., Puma, M.J., 2010. Contribution of soil moisture feedback to hydroclimatic variability. Hydrol. Earth Syst. Sci. 14, 505–520.
Kuzucuoğlu, C., 2009. Climate and environment in times of cultural changes from the 4th to the 1st mill. BC in the Near and Middle East. Scienze dell'Antichità 15 (15), 193–216.
Langgut, D., Finkelstein, I., Litt, T., 2013. Climate and the Late Bronze collapse: new evidence from the southern Levant. Tel Aviv 40 (2), 149–175.
Langgut, D., Adams, M.J., Finkelstein, I., 2016. Climate, settlement patterns and olive horticulture in the southern levant during the early Bronze and intermediate Bronze ages (c. 3600–1950 BC). Levant 48 (2), 117–134.
Lawrence, D., Wilkinson, T.J., 2015. Hubs and upstarts: pathways to urbanism in the northern Fertile Crescent. Antiquity 89 (344), 328–344.
Lawrence, D., Philip, G., Hunt, H., Snape-Kennedy, L., Wilkinson, T.J., 2016. Long term population, city size and climate trends in the Fertile Crescent: a first approximation. PloS One 11 (6), e0157863.
Lawrence, D., Philip, G., Wilkinson, K., Buylaert, J.P., Murray, A.S., Thompson, W., Wilkinson, T.J., 2017. Regional power and local ecologies: accumulated population trends and human impacts in the northern Fertile Crescent. Quat. Int. 437, 60–81.
Lelieveld, J., Hadjinicolaou, P., Kostopoulou, E., Chenoweth, J., El Maayar, M., Giannakopoulos, C., Hannides, C., Lange, M.A., Tanarhte, M., Tyrlis, E., Xoplaki, E.,

2012. Climate change and impacts in the eastern mediterranean and the Middle East. Climatic Change 114 (3–4), 667–687.
Leng, M.J., Marshall, J.D., 2004. Palaeoclimate interpretation of stable isotope data from lake sediment archives. Quat. Sci. Rev. 23 (7–8), 811–831.
Levy, T.E., 1998. Cult, metallurgy and rank societies: Chalcolithic Period (ca. 4500–3500 BCE). In: Levy, T.E. (Ed.), The Archaeology of Society in the Holy Land. Leicester University Press, London, pp. 227–244.
Lotter, A.F., 2003. Multi-proxy climatic reconstructions. In: Mackay, A., Battarbee, R., Birks, J., Oldfield, F. (Eds.), Global Change in the Holocene. Routledge, London, pp. 373–383.
Magee, P., 2014. The Archaeology of Prehistoric Arabia: Adaptation and Social Formation from the Neolithic to the Iron Age. Cambridge University Press, Cambridge.
Manning, K., Colledge, S., Crema, E., Shennan, S., Timpson, A., 2016. The cultural evolution of neolithic europe. EUROEVOL dataset 1: sites, phases and radiocarbon data. J. Open Archaeol. Data 5, e2. https://doi.org/10.5334/joad.40.
Massa, M., Şahoğlu, V., 2015. The 4.2 ka cal. yr. BP climatic event in West and Central Anatolia: combining palaeo-climatic proxies and archaeological data. In: Meller, H., Arz, H.W., Jung, R., et al. (Eds.), *2200 BC – A Climatic Breakdown as a Cause for the Collapse of the Old World?* Halle (Saale): Landesamt für Denkmalpflege und Archäologie Sachsen- Anhalt, Landesmuseum für Vorgeschichte, pp. 61–78.
McMahon, A., 2019. Early urbanism in northern Mesopotamia. J. Archaeol. Res. 1–49 https://doi.org/10.1007/s10814-019-09136-7.
Michczyńska, D.J., Pazdur, A., 2004. Shape analysis of cumulative probability density function of radiocarbon dates set in the study of climate change in late glacial and holocene. Radiocarbon 46 (2), 733–744.
Michczyńska, D.J., Michczyński, A., Pazdur, A., 2007. Frequency distribution of radiocarbon dates as a tool for reconstructing environmental changes. Radiocarbon 49 (2), 799–806.
Moreno, A., Svensson, A., Brooks, S.J., Connor, S., Engels, S., Fletcher, W., Genty, D., Heiri, O., Labuhn, I., Perşoiu, A., Peyron, O., 2014. A compilation of Western European terrestrial records 60–8 ka BP: towards an understanding of latitudinal climatic gradients. Quat. Sci. Rev. 106, 167–185.
Naroll, R., 1956. A preliminary index of social development. Am. Anthropol. 58 (4), 687–715.
Neff, U., Burns, S.J., Mangini, A., Mudelsee, M., Fleitmann, D., Matter, A., 2001. Strong coherence between solar variability and the monsoon in Oman between 9 and 6 kyr ago. Nature 411 (6835), 290.
Nielsen, S.V., Persson, P., Solheim, S., 2019. De-Neolithisation in southern Norway inferred from statistical modelling of radiocarbon dates. J. Anthropol. Archaeol. 53, 82–91.
ORAU, 2016. Oxford Radiocarbon Accelerator Unit (ORAU) Database. Available at: https://c14.arch.ox.ac.uk/.
Ortman, S.G., Andrew, H.F., Cabaniss, J.O.S., Bettencourt, L.M.A., 2014. The prehistory of urban scaling. PloS One 9 (2), e87902.
Orton, D., Morris, J., Pipe, A., 2017. Catch per unit research effort: sampling intensity, chronological uncertainty, and the onset of marine fish consumption in historic London. Open Quat. 3 (1), 1–20.
Palmisano, A., Bevan, A., Shennan, S., 2017. Comparing archaeological proxies for long-term population patterns: an example from central Italy. J. Archaeol. Sci. 87, 59–72.
Palmisano, A., Woodbridge, J., Roberts, C.N., Bevan, A., Fyfe, R., Shennan, S., Cheddadi, R., Greenberg, R., Kaniewski, D., Langgut, D., Leroy, S.A., 2019. Holocene landscape dynamics and long-term population trends in the Levant. Holocene 29 (5), 708–727.
Peltenburg, E.J., 1996. From isolation to state formation in Cyprus c. 3500-1500 BC. In: Karageorghis, V., Michaelides, D. (Eds.), The Development of the Cypriot Economy from the Prehistoric Period to the Present Day. Leventis Foundation, Nicosia, pp. 17–43.
Peltenburg, E.J., 1998. *Excavations at Kissonerga-Mosphilia, 1979–1992*. (2 Vols. Jonsered, Åströms.
Peltenburg, E.J., 2004. Social space in early sedentary communities of Southwest Asia and Cyprus. In: Peltenburg, E.J., Wasse, A. (Eds.), Neolithic Revolution: New Perspectives on Southwest Asia in Light of Recent Discoveries in Cyprus. Oxbow Books, Oxford, pp. 71–90.
Peregrine, P.N., 2004. Cross-cultural approaches in archaeology: comparative ethnology, comparative archaeology, and archaeoethnology. J. Archaeol. Res. 12 (3), 281–309.
Petraglia, M.D., Groucutt, H.S., Guagnin, M., Breeze, P.S., Boivin, N., 2020. Human responses to climate and ecosystem change in ancient Arabia. Proc. Natl. Acad. Sci. Unit. States Am. 117 (15), 8263–8270.
Potts, D.T., 1999. The Archaeology of Elam: Formation and Transformation of an Ancient Iranian State. Cambridge University Press, Cambridge.
Regev, J., De Miroschedji, P., Greenberg, R., Braun, E., Greenhut, Z., Boaretto, E., 2012. Chronology of the Early Bronze Age in the southern Levant: new analysis for a high chronology. Radiocarbon 54 (3–4), 525–566.
Reimer, P.J., Austin, W.E., Bard, E., Bayliss, A., Blackwell, P.G., Ramsey, C.B., et al., 2020. The IntCal20 northern hemisphere radiocarbon age calibration curve (0-55 cal kBP). Radiocarbon 64 (4), 725–757.
Reingruber, A., Thissen, L., 2017. 14SEA: a 14C Database for Southeast Europe and Anatolia (10,000–3000 calBC). Available at: http://www.14sea.org/index.html.
Richerson, P.J., Boyd, R., 2001. Institutional evolution in the Holocene: the rise of complex societies. In: Runciman, W.G. (Ed.), *The Origin of Human Social Institutions*. (Proceedings of the British Academy 110). Oxford University Press, Oxford, pp. 197–234.
Rick, J.W., 1987. Dates as Data: an examination of the Peruvian radiocarbon record. American Anitquity 52, 55–73.
Riehl, S., 2008. Climate and agriculture in the ancient Near East: a synthesis of the archaeobotanical and stable carbon isotope evidence. Veg. Hist. Archaeobotany 17 (1), 43.
Riehl, S., 2012. Variability in ancient Near Eastern environmental and agricultural development. J. Arid Environ. 86, 113–121.
Riehl, S., Pustovoytov, K.E., Weippert, H., Klett, S., Hole, F., 2014. Drought stress variability in ancient Near Eastern agricultural systems evidenced by δ13C in barley grain. Proc. Natl. Acad. Sci. Unit. States Am. 111 (34), 12348–12353.
Roberts, N., Reed, J.M., Leng, M.J., Kuzucuoğlu, C., Fontugne, M., Bertaux, J., Woldring, H., Bottema, S., Black, S., Hunt, E., Karabiyikoğlu, M., 2001. The tempo of Holocene climatic change in the eastern Mediterranean region: new high-resolution crater-lake sediment data from central Turkey. Holocene 11 (6), 721–736.
Roberts, N., Jones, M.D., Benkaddour, A., Eastwood, W.J., Filippi, M.L., Frogley, M.R., Lamb, H.F., Leng, M.J., Reed, J.M., Stein, M., Stevens, L., 2008. Stable isotope records of Late Quaternary climate and hydrology from Mediterranean lakes: the ISOMED synthesis. Quat. Sci. Rev. 27 (25–26), 2426–2441.
Roberts, N., Eastwood, W.J., Kuzucuoğlu, C., Fiorentino, G., Caracuta, V., 2011. Climatic, vegetation and cultural change in the eastern Mediterranean during the mid-Holocene environmental transition. Holocene 21 (1), 147–162.
Roberts, N., Woodbridge, J., Bevan, A., Palmisano, A., Shennan, S., Asouti, E., 2018. Human responses and non-responses to climatic variations during the last Glacial-Interglacial transition in the eastern Mediterranean. Quat. Sci. Rev. 184, 47–67.
Roberts, C.N., Woodbridge, J., Palmisano, A., Bevan, A., Fyfe, R., Shennan, S., 2019. Mediterranean landscape change during the Holocene: synthesis, comparison and regional trends in population, land cover and climate. Holocene 29 (5), 923–937.
Rosen, A.M., 2007. Civilizing Climate: Social Responses to Climate Change in the Ancient Near East. Rowman Altamira Press.
Rowan, Y.M., 2013. The southern levant (cisjordan) during the chalcolithic period. In: Steiner, M.L., Killebrew, A.E. (Eds.), The Oxford Handbook of the Archaeology of the Levant: C. 8000–332 BCE. Oxford University Press, Oxford, pp. 224–236.
Rowe, P.J., Mason, J.E., Andrews, J.E., Marca, A.D., Thomas, L., Van Calsteren, P., Jex, C.N., Vonhof, H.B., Al-Omari, S., 2012. Speleothem isotopic evidence of winter rainfall variability in northeast Turkey between 77 and 6 ka. Quat. Sci. Rev. 45, 60–72.
Sagona, A., 2018. The Archaeology of the Caucasus: from Earliest Settlements to the Iron Age. Cambridge University Press, Cambridge.
Sanders, W.T., 1965. The Cultural Ecology of the Teotihuacan Valley. University Park, Pa.: Dept. of Sociology & Anthropology, Pennsylvania State University.
Savage, S.H., Levy, T.E., 2014. DAAHL—the digital archaeological atlas of the holy land: a model for Mediterranean and world archaeology. Near E. Archaeol. 77 (3), 243–247. Available at: https://daahl.ucsd.edu/DAAHL/.
Schwartz, G.M., 2017. Western Syria and the third- to second-millennium B.C. In: Höflmayer, F. (Ed.), The Late Third Millennium in the Ancient Near East: Chronology, C14, and Climate Change. University of Chicago Press, Chicago, pp. 87–130.
Shah, A.M., Morrill, C., Gille, E.P., Gross, W.S., Anderson, D.M., Bauer, B.A., Buckner, R., Hartman, M., 2013. Global Speleothem Oxygen Isotope Measurements since the Last Glacial Maximum. Dataset Papers in Science, 2013. https://doi.org/10.7167/2013/548048.
Shennan, S., 2000. Population, culture history, and the dynamics of culture change. Curr. Anthropol. 41, 811–835.
Shennan, S., 2018. The First Farmers of Europe: an Evolutionary Perspective. Cambridge University Press, Cambridge.
Shennan, S., Edinborough, K., 2007. Prehistoric population history: from the late glacial to the late neolithic in central and northern europe. J. Archaeol. Sci. 34, 1339–1345.
Shennan, S., Downey, S.S., Timpson, A., Edinborough, K., Colledge, S., Kerig, T., Manning, K., Thomas, M.G., 2013. Regional population collapse followed initial agriculture booms in mid-Holocene Europe. Nat. Commun. 4 (1), 1–8.
Silva, F., Vander Linden, M., 2017. Amplitude of travelling front as inferred from 14 C predicts levels of genetic admixture among European early farmers. Sci. Rep. 7 (1), 1–9.
Simmons, A., 2011. Re-writing the Colonisation of Cyprus: Tales of Hippo Hunters and Cow Herders. In: Phoca- Cosmetatou, N. (Ed.), The First Mediterranean Islanders: Initial Occupation and Survival Strategies. University of Oxford School of Archaeology, Oxford, pp. 55–75.
Sinha, A., Kathayat, G., Weiss, H., Li, H., Cheng, H., Reuter, J., Schneider, A.W., Berkelhammer, M., Adalı, S.F., Stott, L.D., Edwards, R.L., 2019. Role of climate in the rise and fall of the Neo-Assyrian Empire. Science advances 5 (11), eaax6656.
Smith, M.E., 2019. Energized crowding and the generative role of settlement aggregation and urbanization. In: Gyucha, A. (Ed.), Coming Together: Comparative Approaches to Population Aggregation and Early Urbanization. State University of New York Press, Albany, pp. 37–58.
Steel, L., 2013. Cyprus during the late Bronze age. In: The Oxford Handbook of the Archaeology of the Levant: C. 8000–332 BCE. Oxford University Press, Oxford, pp. 865–886.
Stein, M., Torfstein, A., Gavrieli, I., Yechieli, Y., 2010. Abrupt aridities and salt deposition in the post-glacial Dead Sea and their North Atlantic connection. Quat. Sci. Rev. 29 (3–4), 567–575.

Stephens, L., Fuller, D., Boivin, N., Rick, T., Gauthier, N., Kay, A., Marwick, B., Geralda, C., Armstrong, D., Barton, C.M., Denham, T., et al., 2019. Archaeological assessment reveals Earth's early transformation through land use. Science 365 (6456), 897–902.
Stevens, L.R., Wright Jr., H.E., Ito, E., 2001. Proposed changes in seasonality of climate during the lateglacial and holocene at Lake Zeribar, Iran. Holocene 11 (6), 747–755.
Stevens, L.R., Ito, E., Schwalb, A., Wright, H.E., 2006. Timing of atmospheric precipitation in the Zagros Mountains inferred from a multi-proxy record from Lake Mirabad, Iran. Quat. Res. 66 (3), 494–500.
Stiner, M.C., Buitenhuis, H., Duru, G., Kuhn, S.L., Mentzer, S.M., Munro, N.D., Pöllath, N., Quade, J., Tsartsidou, G., Özbaşaran, M., 2014. A forager–herder trade-off, from broad-spectrum hunting to sheep management at Aşıklı Höyük, Turkey. Proc. Natl. Acad. Sci. Unit. States Am. 111 (23), 8404–8409.
Stoddart, S., Woodbridge, J., Palmisano, A., Mercuri, A.M., Mensing, S.A., Colombaroli, D., Sadori, L., Magri, D., Di Rita, F., Giardini, M., Mariotti Lippi, M., 2019. Tyrrhenian central Italy: holocene population and landscape ecology. Holocene 29 (5), 761–775.
Tallavaara, M., Pesonen, P., Oinonen, M., 2010. Prehistoric population history in eastern Fennoscandia. J. Archaeol. Sci. 37 (2), 251–260.
TAY project, 2019. 14C Database (22nd Update). Available at: http://tayproject.org/C14searcheng.html.
Thomas, E.R., Wolff, E.W., Mulvaney, R., Steffensen, J.P., Johnsen, S.J., Arrowsmith, C., White, J.W., Vaughn, B., Popp, T., 2007. The 8.2 ka event from Greenland ice cores. Quat. Sci. Rev. 26 (1–2), 70–81.
Timpson, A., Colledge, S., Crema, E., Edinborough, K., Kerig, T., Manning, K., Thomas, M.G., Shennan, S., 2014. Reconstructing regional population fluctuations in the European Neolithic using radiocarbon dates: a new case-study using an improved method. J. Archaeol. Sci. 52, 549–557.
Torfing, T., 2015. Layers of assumptions: a reply to Timpson, Manning, and shennan. J. Archaeol. Sci. 63, 203–205.
Torfing, T., 2016. Demographic proxies for the neolithic: with emphasis on the langeland region, Denmark. Acta Archaeol. 87 (1), 33–48.
Turchin, P., 2001. Does population ecology have general laws? Oikos 94 (1), 17–26.
Turchin, P., Nefedov, S.A., 2009. Secular Cycles. Princeton University Press, Princeton.
Ünal-İmer, E., Shulmeister, J., Zhao, J.X., Uysal, I.T., Feng, Y.X., Nguyen, A.D., Yüce, G., 2015. An 80 kyr-long continuous speleothem record from Dim Cave, SW Turkey with paleoclimatic implications for the Eastern Mediterranean. Sci. Rep. 5 (1), 1–11.
Ur, J.A., 2009. Emergent landscapes of movement in early Bronze age northern Mesopotamia. In: Snead, J.E., Erickson, C., Darling, A.W. (Eds.), Landscapes of Movement: Paths, Trails, and Roads in Anthropological Perspective. University of Pennsylvania Museum Press, Philadelphia, pp. 180–203.
Ur, J.A., 2010. Cycles of civilization in northern Mesopotamia, 4400–2000 BC. J. Archaeol. Res. 18 (4), 387–431.
Ur, J., 2013. Patterns of settlement in sumer and akkad. In: Crawford, H.E. (Ed.), The Sumerian World. Routledge, London, pp. 155–179.
Ur, J.A., 2015. Urban adaptations to climate change in northern Mesopotamia. In: Kerner, S., Dann, R., Bangsgaard, P. (Eds.), Climate and Ancient Societies. Museum Tusculanum Press, Copenhagen, pp. 69–95.
Van Strydonck, M., De Roock, E., 2011. Royal institute for cultural heritage web-based radiocarbon database. Radiocarbon 53 (2), 367–370. Available at: http://c14.kikirpa.be/.
Walker, M., Head, M.J., Berkelhammer, M., Björck, S., Cheng, H., Cwynar, L., Fisher, D., Gkinis, V., Long, A., Lowe, J., Newnham, R., 2018. Formal ratification of the subdivision of the holocene series/epoch (quaternary system/period): two new global boundary stratotype sections and points (GSSPs) and three new stages/subseries. Episodes 41 (4), 213–223.
Wassenburg, J.A., Dietrich, S., Fietzke, J., Fohlmeister, J., Jochum, K.P., Scholz, D., Richter, D.K., Sabaoui, A., Spötl, C., Lohmann, G., Andreae, M.O., 2016. Reorganization of the north atlantic oscillation during early holocene deglaciation. Nat. Geosci. 9 (8), 602–605.
Webb, J., 2014. Cyprus during the early Bronze age. In: Steiner, M.L., Killebrew, A.E. (Eds.), The Oxford Handbook of the Archaeology of the Levant: C. 8000–332 BCE. Oxford University Press, Oxford, pp. 532–551.
Weiberg, E., Bevan, A., Kouli, K., Katsianis, M., Woodbridge, J., Bonnier, A., Engel, M., Finné, M., Fyfe, R., Maniatis, Y., Palmisano, A., 2019. Long-term trends of land use and demography in Greece: a comparative study. Holocene 29 (5), 742–760.
Weiss, H., 2016. Global megadrought, societal collapse and resilience at 4.2–3.9 ka BP across the Mediterranean and west Asia. Magazine 24 (2), 62–63.
Weiss, H., 2017. 4.2 ka BP Megadrought and the Akkadian collapse. In: Weiss, H. (Ed.), Megadrought and Collapse: from Early Agriculture to Angkor. Oxford University Press, Oxford, pp. 93–160.
Weiss, H., Courty, M.-A., Wetterstrom, W., Guichard, F., Senior, L., Meadow, R., Curnow, A., 1993. The genesis and collapse of third millennium north Mesopotamian civilization. Science 261 (5124), 995–1004.
Weninger, B.P., 2017. Niche construction and theory of agricultural origins. Case studies in punctuated equilibrium. Documenta Praehistorica 44, 6–17.
Weninger, B., 2018. CalPal Archaeological 14C-Database. Available at: https://www.academia.edu/36766067/CalPal_Archaeological_14C-Database_Europe.xlsx_June_2018. (Accessed 20 November 2019).
Weninger, B., Clare, L., Rohling, E., Bar-Yosef, O., Böhner, U., Budja, M., Bundschuh, M., Feurdean, A., Gebe, H.G., Jöris, O., Linstädter, J., 2009. The impact of rapid climate change on prehistoric societies during the Holocene in the Eastern Mediterranean. Documenta praehistorica 36, 7–59.
Weninger, B., Clare, L., Jöris, O., Jung, R., Edinborough, K., 2015. Quantum theory of radiocarbon calibration. World Archaeol. 47 (4), 543–566.
Wick, L., Lemcke, G., Sturm, M., 2003. Evidence of Lateglacial and Holocene climatic change and human impact in eastern Anatolia: high-resolution pollen, charcoal, isotopic and geochemical records from the laminated sediments of Lake Van, Turkey. Holocene 13 (5), 665–675.
Wilkinson, T.J., 1997. Environmental fluctuations, agricultural production and collapse: a view from Bronze Age Upper Mesopotamia. In: Dalfes, H.N., Kukla, G., Weiss, H. (Eds.), Third Millennium BC Climate Change and Old World Collapse. Springer-Verlag, Berlin, pp. 67–106.
Wilkinson, T., 1999. Demographic trends from archaeological survey: case studies from the Levant and Near East. In: Bintliff, J., Sbonias, K. (Eds.), Reconstructing Past Population Trends in Mediterranean Europe (3000 BC-AD 1800). Oxbow Books, Oxford, pp. 45–64.
Wilkinson, T.J., 2003. Archaeological Landscapes of the Near East. University of Arizona Press, Tucson, AZ.
Wilkinson, T.J., Ur, J., Wilkinson, E.B., Altaweel, M., 2005. Landscape and settlement in the neo-assyrian empire. Bull. Am. Sch. Orient. Res. 340, 23–56.
Wilkinson, T.J., Christiansen, J., Ur, J.A., Widell, M., Altaweel, M., 2007. Urbanization within a dynamic environment: modelling Bronze age communities in upper Mesopotamia. Am. Anthropol. 109 (1), 52–68.
Wilkinson, T.J., Philip, G., Bradbury, J., Dunford, R., Donoghue, D., Galiatsatos, N., Lawrence, D., Ricci, A., Smith, S.L., 2014. Contextualizing early urbanization: settlement cores, early states and agro-pastoral strategies in the Fertile Crescent during the fourth and third millennia BC. J. World PreHistory 27 (1), 43–109.
Williams, A.N., 2012. The use of summed radiocarbon probability distributions in archaeology: a review of methods. J. Archaeol. Sci. 39 (3), 578–589.
Woodbridge, J., Roberts, C.N., Palmisano, A., Bevan, A., Shennan, S., Fyfe, R., Eastwood, W.J., Izdebski, A., Çakırlar, C., Woldring, H., Broothaerts, N., 2019. Pollen-inferred regional vegetation patterns and demographic change in Southern Anatolia through the Holocene. Holocene 29 (5), 728–741.
Wright, H.T., Johnson, G.A., 1975. Population, exchange, and early state formation in southwestern Iran. Am. Anthropol. 77 (2), 267–289.
Yakar, J., 1993. Anatolian Civilization following the disintegration of the Hittite Empire: an archaeological appraisal. Tel Aviv 20 (1), 3–28.
Zeder, M.A., 2005. A view from the Zagros: new perspectives on livestock domestication in the Fertile Crescent. In: Vigne, J.D., Peters, J., Helmer, D. (Eds.), The First Steps of Animal Domestication: New Archaeological Approaches. Oxbow Books, Oxford, pp. 125–146.
Zielhofer, C., Köhler, A., Mischke, S., Benkaddour, A., Mikdad, A., Fletcher, W.J., 2019. Western Mediterranean hydro-climatic consequences of Holocene ice-rafted debris (Bond) events. Clim. Past 15 (2), 463–475.